

# Linear seesaw in $A'_5$ modular symmetry with Leptogenesis

Mitesh Kumar Behera\* and Rukmani Mohanta†

*School of Physics, University of Hyderabad, Hyderabad - 500046, India*

## Abstract

In this paper, we investigate the implication of modular  $\Gamma'_5 \simeq A'_5$  symmetry on neutrino oscillation phenomenology in the linear seesaw framework. In order to achieve the well defined mass structure for the light active neutrinos as dictated by the linear seesaw mechanism, we introduce six heavy fermion fields along with a pair of weightons to retain the holomorphic nature of the superpotential. The notable feature of modular symmetry is that, it reduces the usage of flavon fields significantly. In addition, the Yukawa couplings transform non-trivially under the flavor symmetry group and expressed in terms of the Dedekind eta functions, the  $q$  expansion of which renders numerical simplicity in calculations. We demonstrate that the model framework diligently accommodates all the neutrino oscillation data. Alongside, we also investigate the effect of CP asymmetry generated from the decay of lightest heavy fermions to explain the observed baryon asymmetry through the phenomenon of leptogenesis.

arXiv:2201.10429v2 [hep-ph] 29 Mar 2022

---

\*Electronic address: miteshbehera1304@gmail.com

†Electronic address: rmsp@uohyd.ac.in

## I. INTRODUCTION

There are several unsolved knots in the realm of particle physics, e.g., the baryon asymmetry of the Universe, the dark matter content, the origin of neutrino masses and mixing, etc., and the understanding of these issues is one of the prime objectives of the present day research. In the last couple of decades, several diligent attempts have been made towards comprehending and resolving the issue of dynamical origin of fermion masses and their mixing. Present scenario has taken us few steps ahead in terms of getting a convincing explanation of the origin of mass through Higgs mechanism while being within the domain of Standard Model (SM). However, it does not provide proper grounds to explain the origin of the observed neutrino masses and their mixing. Rather, very diverse approaches are made in order to gain an insightful resolution towards the above existing problems, and obviously the answer lies in going beyond standard model (BSM) physics. It should be emphasized that, certain well-defined patterns are observed in quark masses and mixing, the appreciation of which is still an enigma. Nonetheless, there are ample amount of research work present, which make an attempt to grasp their fundamental origin. In addition, perplexity to the problem has increased due to the observation of the neutrino masses and their sizeable mixing. The reason being, the order of magnitude of the observed neutrino masses are approximately twelve order smaller than that of EW scale. Also, there is immense difference in the pattern of leptonic and quark mixings, the former is having large mixing angles, while the later involves smaller mixing angles. Numerous experiments [1–4] have confirmed the tininess of the neutrino mass and other parameters with high accuracy. The best-fit values of the neutrino oscillation parameters are furnished in Refs. [5, 6].

It is well-known that in the SM framework, the neutrino mass generation can not be explained through the standard Higgs mechanism due to the absence of the right-handed (RH) components. Still, if we could manage to add the RH neutrinos into SM by hand, and allow Dirac mass terms, the values of the required Yukawa couplings to be around  $\mathcal{O}(10^{-12})$ , which appear as aberrant. In contrast, there exist many BSM scenarios that help to generate tiny neutrino mass through the conventional seesaw mechanism. Some of the prominent seesaw mechanisms are categorized as type-I [7–10], type-II [11–16], type-III [17–22] and all of them require additional heavy fermions or scalars beyond the SM particle content. Literature survey shows there are many flavor symmetries either discrete  $A_4$  [23–25],  $S_3$  [26–29],  $S_4$  [30–32] etc. or continuous  $U(1)_{B-L}$  [33–37],  $U(1)_H$  [38–40],  $U(1)_{L_e-L_\tau}$  [41, 42] etc., which can generate the tiny neutrino masses and also accommodate the observed neutrino oscillation data with the help of some additional scalars and perturbation (wherever required). As aforesaid, inclusion of flavons affects the neatness of the model and the predictability of the model is hampered because of the higher dimensional operators. These drawbacks can be eliminated through the recent approach of including modular symmetry [43–66], where the Yukawa couplings transform non-trivially under the discrete flavor symmetry group and have certain modular weight.

The modular group  $\Gamma'_5 \simeq A'_5$  is a new and promising candidate, which corresponds to the specific case of  $N = 5$ . People have done extensive studies on the basic properties of this finite group  $A'_5$  [67–69], so here we bring up only the important points regarding  $A'_5$  modular symmetry. The  $A'_5$  group consists of 120 elements, which are likely to be produced by the generators  $S, T$  and  $R$  gratifying the identities for  $N = 5$  [70]. So, categorization of these 120 elements are done into nine conjugacy classes which are represented by nine well defined irreducible representations, symbolized as  $\mathbf{1}, \widehat{\mathbf{2}}, \widehat{\mathbf{2}}', \mathbf{3}, \mathbf{3}', \mathbf{4}, \widehat{\mathbf{4}}, \mathbf{5}$  and  $\widehat{\mathbf{6}}$ . Additionally, the conjugacy classes and character table of  $A'_5$ , as well as the representation matrices of all three generators  $S, T$  and  $R$ , are presented in Appendix [70]. It ought to be noticed that the  $\mathbf{1}, \mathbf{3}, \mathbf{3}', \mathbf{4}$  and  $\mathbf{5}$  representations with  $R = \mathbb{I}$  coincide with those for  $A_5$ , while  $\widehat{\mathbf{2}}, \widehat{\mathbf{2}}', \widehat{\mathbf{4}}$  and  $\widehat{\mathbf{6}}$  are unique for  $A'_5$  with  $R = -\mathbb{I}$ . As we are working in the modular space of  $\Gamma(5)$ , hence, its dimension is  $5k + 1$ , where,  $k$  is the modular weight. A brief discussion concerning the modular space of  $\Gamma(5)$  is presented in Appendix A. For  $k = 1$ , the modular space  $M_1[\Gamma(5)]$  will have six basis vectors i.e.,  $(\widehat{e}_i, \text{ where } i = 1, 2, 3, 4, 5, 6)$  whose  $q$ -expansion are given below and they are used in expressing the Yukawa coupling  $Y_{\widehat{\mathbf{6}}}^{(1)}$  as shown in Appendix B:

$$\begin{aligned}
\widehat{e}_1 &= 1 + 3q + 4q^2 + 2q^3 + q^4 + 3q^5 + 6q^6 + 4q^7 - q^9 + \dots, \\
\widehat{e}_2 &= q^{1/5} (1 + 2q + 2q^2 + q^3 + 2q^4 + 2q^5 + 2q^6 + q^7 + 2q^8 + 2q^9 + \dots), \\
\widehat{e}_3 &= q^{2/5} (1 + q + q^2 + q^3 + 2q^4 + q^6 + q^7 + 2q^8 + q^9 + \dots), \\
\widehat{e}_4 &= q^{3/5} (1 + q^2 + q^3 + q^4 - q^5 + 2q^6 + 2q^8 + q^9 + \dots), \\
\widehat{e}_5 &= q^{4/5} (1 - q + 2q^2 + 2q^6 - 2q^7 + 2q^8 + q^9 + \dots), \\
\widehat{e}_6 &= q (1 - 2q + 4q^2 - 3q^3 + q^4 + 2q^5 - 2q^6 + 3q^8 - 2q^9 + \dots),
\end{aligned} \tag{1}$$

where  $q \equiv e^{2i\pi\tau}$ , with  $\tau$  as a complex modulus parameter. The significance of the modulus  $\tau$  is that, the modular group  $\Gamma$  is generated by performing the linear fractional transformation on  $\tau$  as follows

$$\gamma : \tau \rightarrow \gamma(\tau) \rightarrow \frac{a\tau + b}{c\tau + d}, \{a, b, c, d \in Z : ad - bc = 1, \text{Im}\tau > 0\}. \tag{2}$$

Our aim here is to utilize the expediency of  $A'_5$  modular symmetry by employing it to linear seesaw mechanism in the context of supersymmetry, as we are quite familiar with the dynamics of TeV scale seesaw frameworks from numerous [71, 72] literature. The deciding factor whether it will be linear seesaw or inverse seesaw is the position of the zero elements in the mass matrix under the basis of  $(\nu, N_{R_i}, S_{L_i})$ . It is quite evident when 11 and 33 elements of the mass matrix are zero, it gives the structure of linear seesaw. As mentioned above, introduction of three left-handed neutral fermions superfields  $S_{L_i}$  alongside three-right handed ones  $N_{R_i}$  ( $i = 1, 2, 3$ ) validates and produces the neutrino mass matrix structure of linear seesaw which is intricate enough, and has been studied in the context of discrete  $A_4$  flavor symmetry in [73–75]. In this work, we are implementing it under  $A'_5$  modular

symmetry. For this purpose, the heavy fermions  $S_{Li}$  &  $N_{Ri}$  are assigned as  $3'$  under  $A'_5$  symmetry and modular form of the Yukawa couplings leads to a constrained structure. After that we perform the numerical analysis to look for the region which is acceptable in order to fit the neutrino data. Hence, prediction for the neutrino sector is done after fixing the allowed parameter space.

Structure of this paper is as follows. In Sec. II we discuss the layout of the familiar linear seesaw framework with  $A'_5$  modular symmetry and its alluring feature, which leads to simple mass structure for the charged-leptons as well as neutral leptons, utilizing the product rules of  $A'_5$  symmetry. We thereafter, briefly discuss the phenomena of light neutrino masses and mixing in this framework. The numerical analysis pertaining to different observables of neutrino sector and the input model parameters is presented in Sec. III. We also briefly comment on the non-unitarity effect. The discussion on leptogenesis within the context of the proposed model is furnished in Sec. IV and our results are summarized in Sec. V.

## II. MODEL FRAMEWORK

<b>Fields</b>	$e_R^c$	$\mu_R^c$	$\tau_R^c$	$L_L$	$N_R^c$	$S_L$	$H_{u,d}$	$\zeta$	$\zeta'$
$SU(2)_L$	1	1	1	2	1	1	2	1	1
$U(1)_Y$	1	1	1	$-\frac{1}{2}$	0	0	$\frac{1}{2}, -\frac{1}{2}$	0	0
$U(1)_{B-L}$	1	1	1	-1	1	0	0	1	-1
$A'_5$	1	1	1	3	$3'$	$3'$	1	1	1
$k_I$	1	3	5	1	1	4	0	1	1

TABLE I: The particle spectrum and their charges under the symmetry groups  $SU(2)_L \times U(1)_Y \times U(1)_{B-L} \times A'_5$  while  $k_I$  represents the modular weight.

Here we work on a model under linear seesaw scenario in the context of supersymmetry (SUSY), where Table I provided below expresses the particle content and their respective group charges. For exploring neutrino sector beyond standard model (BSM), we extend it with the discrete  $A'_5$  modular symmetry and a local  $U(1)_{B-L}$  gauge symmetry. However, the local  $U(1)_{B-L}$  becomes the auxillary symmetry which has been added to avoid certain undesirable terms in the superpotential. The advantage of working in BSM is that we can add right handed neutrinos and extra fields, and hence, here we have included three extra right-handed SM singlet superfields ( $N_{Ri}$ ), three left handed singlet superfields ( $S_{Li}$ ) and a pair weightons ( $\zeta, \zeta'$ ) in the particle gamut. The transformation of extra added superfields is taken as  $3'$  under the  $A'_5$  modular group. The  $A'_5$  and  $U(1)_{B-L}$  symmetries are broken at a very high scale, much greater than the scale of electroweak symmetry breaking [76].

Mass acquisition by the extra singlet superfield happens by allocating non-zero vacuum expectation values (VEVs) to the weightons  $\zeta$  and  $\zeta'$ . The modular weight assigned to various particles is denoted by  $k_I$ . One of the significant point of introducing modular symmetry is the curtailment of flavon (weighton) fields, which otherwise are traditionally required while working in BSM with discrete symmetries, since the Yukawa couplings have non-trivial group transformation under  $A'_5$  modular symmetry group, and their transformation are present in [70].

The complete superpotential is given by

$$\begin{aligned} \mathcal{W} = & A_{M_l} \left[ (L_L l_R^c)_3 Y_3^{k_Y} \right] H_d + \mu H_u H_d + G_D \left[ (L_L N_R^c)_5 Y_5^{(2)} \right] H_u + \\ & G_{LS} \left[ (L_L S_L)_4 H_u \sum_{i=1}^2 Y_{4,i}^{(6)} \right] \frac{\zeta}{\Lambda} + B_{M_{RS}} \left[ (S_L N_R^c)_5 \sum_{i=1}^2 Y_{5,i}^{(6)} \right] \zeta'. \end{aligned} \quad (3)$$

where,  $A_{M_l} = (\alpha_{M_l}, \beta_{M_l}, \gamma_{M_l})$ ,  $l_R^c = (e_R^c, \mu_R^c, \tau_R^c)$ ,  $k_Y = (2, 4, 6)$ , and  $G_D = \text{diag}\{g_{D_1}, g_{D_2}, g_{D_3}\}$ ,  $G_{LS} = \text{diag}\{g_{LS_1}, g_{LS_2}, g_{LS_3}\}$ ,  $B_{M_{RS}} = \text{diag}\{\alpha_{RS_1}, \alpha_{RS_2}, \alpha_{RS_3}\}$  represent the coupling strengths of various interaction terms.

### A. Mass terms for the charged leptons ( $M_\ell$ )

In order to have a clear and simplified structure for charged lepton mass matrix, we consider the three families of left-handed lepton doublets ( $L_L$ ) to transform as 3 under the  $A'_5$  symmetry with  $U(1)_{B-L}$  charge  $-1$ . The right-handed charged leptons  $N_R^c$  transform as singlets under  $A'_5$  symmetry and have  $U(1)_{B-L}$  charge  $+1$ . However,  $(e_R^c, \mu_R^c, \tau_R^c)$  are given the modular weight as 1, 3, 5 respectively. The Higgsinos  $H_{u,d}$  are given charges 0, 1 under the  $U_{B-L}$  and  $A'_5$  symmetries with zero modular weights. The VEVs of these Higgsinos  $H_u$  and  $H_d$  are given as  $v_u/\sqrt{2}$  and  $v_d/\sqrt{2}$  respectively. Moreover, Higgsinos VEVs are associated to SM Higgs VEV as  $v_H = \frac{1}{2}\sqrt{v_u^2 + v_d^2}$  and the ratio of their VEVs is expressed as  $\tan \beta = (v_u/v_d)$  and we use its value to be 5 in our analysis. The relevant superpotential terms for charged leptons obtained from (4) are given as

$$\mathcal{W}_{M_l} = \alpha_{M_l} \left[ (L_L e_R^c)_3 Y_3^{(2)} \right] H_d + \beta_{M_l} \left[ (L_L \mu_R^c)_3 Y_3^{(4)} \right] H_d + \gamma_{M_l} \left[ (L_L \tau_R^c)_3 \left\{ \sum_{i=1}^2 Y_{3,i}^{(6)} \right\} \right] H_d \quad (4)$$

Working under  $A'_5$  modular group, its Kronecker product (as provided in Appendix C), leaves us with a non diagonal charged lepton mass matrix after the spontaneous symmetry

breaking. The mass matrix takes the form

$$M_l = \frac{v_d}{\sqrt{2}} \begin{bmatrix} \left( Y_{\mathbf{3}}^{(2)} \right)_1 \left( Y_{\mathbf{3}}^{(4)} \right)_1 \left( \sum_{i=1}^2 Y_{\mathbf{3},i}^{(6)} \right)_1 \\ \left( Y_{\mathbf{3}}^{(2)} \right)_3 \left( Y_{\mathbf{3}}^{(4)} \right)_3 \left( \sum_{i=1}^2 Y_{\mathbf{3},i}^{(6)} \right)_3 \\ \left( Y_{\mathbf{3}}^{(2)} \right)_2 \left( Y_{\mathbf{3}}^{(4)} \right)_2 \left( \sum_{i=1}^2 Y_{\mathbf{3},i}^{(6)} \right)_2 \end{bmatrix}_{LR} \cdot \begin{bmatrix} \alpha_{M_l} & 0 & 0 \\ 0 & \beta_{M_l} & 0 \\ 0 & 0 & \gamma_{M_l} \end{bmatrix}. \quad (5)$$

The charged lepton mass matrix  $M_l$  can be diagonalised by the unitary matrix  $U_l$ , giving rise to the physical masses  $m_e$ ,  $m_\mu$  and  $m_\tau$  as

$$U_l^\dagger M_l M_l^\dagger U_l = \text{diag}(m_e^2, m_\mu^2, m_\tau^2). \quad (6)$$

In addition, it also satisfies the following identities, which will be used for numerical analysis in section III:

$$\begin{aligned} \text{Tr} \left( M_l M_l^\dagger \right) &= m_e^2 + m_\mu^2 + m_\tau^2, \\ \text{Det} \left( M_l M_l^\dagger \right) &= m_e^2 m_\mu^2 m_\tau^2, \\ \frac{1}{2} \left[ \text{Tr} \left( M_l M_l^\dagger \right) \right]^2 - \frac{1}{2} \text{Tr} \left[ \left( M_l M_l^\dagger \right)^2 \right] &= m_e^2 m_\mu^2 + m_\mu^2 m_\tau^2 + m_\tau^2 m_e^2. \end{aligned} \quad (7)$$

## B. Dirac and pseudo-Dirac mass terms for the light neutrinos

In addition to lepton doublets transformation, hitherto, the heavy fermion superfields, i.e.,  $N_{R_i}$  ( $S_{L_i}$ ) transform as triplet  $3'$  under  $A_5$  modular group with  $U(1)_{B-L}$  charge of  $-1$  ( $0$ ) along with modular weight 1 ( $4$ ) respectively. As discussed in Ref. [70], the choice of Yukawa couplings depends on the equation  $k_Y = k_{I_1} + k_{I_2} + \dots + k_{I_n}$  where  $k_Y$  is the modular weight of Yukawa couplings and  $\sum_{i=1}^n k_{I_n}$  is sum of the modular weights of all other particles present in the definition of superpotential terms. These Yukawa couplings are expressed in terms of Dedekind eta-function  $\eta(\tau)$ , and thus have  $q$ -expansion forms, in order to avoid the complexity in calculations. The relevant superpotential term involving the active and right-handed neutrinos can be expressed as

$$\mathcal{W}_D = G_D \left[ (L_L N_R^c)_5 Y_5^{(2)} \right] H_u, \quad (8)$$

where,  $G_D$  is the diagonal matrix containing the free parameters and the modular weight of the Yukawa coupling is equal to the sum of the the modular weights of all other particles present in (8). The choice of the Yukawa coupling is made based on the Kroncker product rules for  $A_5$  modular symmetry such that superpotential remains singlet. The resulting

Dirac neutrino mass matrix is found to be

$$M_D = \frac{v_u}{\sqrt{30}} G_D \begin{bmatrix} \sqrt{3}(Y_5^{(2)})_1 & (Y_5^{(2)})_4 & (Y_5^{(2)})_3 \\ (Y_5^{(2)})_5 & -\sqrt{2}(Y_5^{(2)})_3 & -\sqrt{2}(Y_5^{(2)})_2 \\ (Y_5^{(2)})_2 & -\sqrt{2}(Y_5^{(2)})_5 & -\sqrt{2}(Y_5^{(2)})_4 \end{bmatrix}_{LR}. \quad (9)$$

As the transformation of the sterile fermion superfield  $S_L$  is same as  $N_R$  under  $A'_5$  modular symmetry, it allows us to define a pseudo-Dirac mass term for the light neutrinos and the corresponding interaction superpotential is expressed as

$$\mathcal{W}_{LS} = G_{LS} \left[ (L_L S_L)_4 \sum_2^{i=1} Y_{4,i}^{(6)} \right] H_u \left( \frac{\zeta}{\Lambda} \right), \quad (10)$$

where,  $G_{LS}$  is a diagonal matrix containing three free parameters and the choice of Yukawa coupling depends upon the idea of keeping the superpotential singlet. Thus, we obtain the structure for the pseudo-Dirac neutrino mass matrix of the form,

$$M_{LS} = \frac{v_u}{2\sqrt{6}} \left( \frac{v_\zeta}{\sqrt{2}\Lambda} \right) G_{LS} \begin{bmatrix} 0 & -\sqrt{2} \left( \sum_{i=1}^2 Y_{4,i}^{(6)} \right)_3 & -\sqrt{2} \left( \sum_{i=1}^2 Y_{4,i}^{(6)} \right)_2 \\ \sqrt{2} \left( \sum_{i=1}^2 Y_{4,i}^{(6)} \right)_4 & - \left( \sum_{i=1}^2 Y_{4,i}^{(6)} \right)_2 & \left( \sum_{i=1}^2 Y_{4,i}^{(6)} \right)_1 \\ \left( \sum_{i=1}^2 Y_{4,i}^{(6)} \right)_1 & \left( \sum_{i=1}^2 Y_{4,i}^{(6)} \right)_4 & - \left( \sum_{i=1}^2 Y_{4,i}^{(6)} \right)_3 \end{bmatrix}_{LR}. \quad (11)$$

### C. Mixing between the heavy fermions $N_{Ri}$ and $S_{Li}$

Introduction of extra symmetries, helps in allowing the mixing of heavy superfields but forbids the usual Majorana mass terms. Hence, below we exhibit the mixing of these extra superfields i.e.,  $(N_R, S_L)$  as follows

$$\mathcal{W}_{MRS} = B_{MRS} \left[ (S_L N_R^c)_5 \sum_{i=1}^2 Y_{5,i}^{(6)} \right] \zeta', \quad (12)$$

where,  $B_{MRS}$  is the free parameter &  $\langle \zeta' \rangle = v_{\zeta'}/\sqrt{2}$  is the VEV of  $\zeta'$  and the superpotential is singlet under the  $A'_5$  modular symmetry product rule. Thus, considering  $v_{\zeta'} \approx v_\zeta$ , one can obtain the mass matrix as follows:

$$M_{RS} = \frac{v_\zeta}{\sqrt{60}} B_{MRS} \begin{bmatrix} 2 \left( \sum_{i=1}^2 Y_{5,i}^{(6)} \right)_1 & -\sqrt{3} \left( \sum_{i=1}^2 Y_{5,i}^{(6)} \right)_4 & -\sqrt{3} \left( \sum_{i=1}^2 Y_{5,i}^{(6)} \right)_3 \\ -\sqrt{3} \left( \sum_{i=1}^2 Y_{5,i}^{(6)} \right)_4 & \sqrt{6} \left( \sum_{i=1}^2 Y_{5,i}^{(6)} \right)_2 & - \left( \sum_{i=1}^2 Y_{5,i}^{(6)} \right)_1 \\ -\sqrt{3} \left( \sum_{i=1}^2 Y_{5,i}^{(6)} \right)_3 & - \left( \sum_{i=1}^2 Y_{5,i}^{(6)} \right)_1 & \sqrt{6} \left( \sum_{i=1}^2 Y_{5,i}^{(6)} \right)_5 \end{bmatrix}_{LR}. \quad (13)$$

The masses for the heavy superfields can be found in the basis  $(N_R, S_L)^T$  as

$$M_{hf} = \begin{pmatrix} 0 & M_{RS} \\ M_{RS}^T & 0 \end{pmatrix}. \quad (14)$$

Hence, one can have three doubly degenerate mass eigenstates for the heavy superfields upon diagonalization.

#### D. Linear Seesaw framework for the light neutrino masses

In the present scenario of  $A'_5$  modular symmetry, the light neutrino masses can be generated in the framework of linear seesaw. Thus, the mass matrix in the flavor basis of  $(\nu_L, N_R^c, S_L)^T$ , can be manifested as

$$\mathbb{M} = \begin{pmatrix} \nu_L & N_R^c & S_L \\ \nu_L & 0 & M_D & M_{LS} \\ N_R^c & M_D^T & 0 & M_{RS} \\ S_L & M_{LS}^T & M_{RS}^T & 0 \end{pmatrix}. \quad (15)$$

The mass formula for the light neutrinos in the framework of linear seesaw is governed by the assumption that  $M_{RS} \gg M_D, M_{LS}$  and is given as

$$m_\nu = M_D M_{RS}^{-1} M_{LS}^T + \text{transpose}. \quad (16)$$

Besides the light neutrino masses, other related parameters in the leptonic sector are the Jarlskog invariant, which signifies the measure of CP violation and the effective neutrino mass parameter  $m_{ee}$  that plays a key role in the neutrinoless double beta decay process. These parameters can be obtained from the PMNS matrix elements through the following relations:

$$J_{CP} = \text{Im}[U_{e1}U_{\mu 2}U_{e2}^*U_{\mu 1}^*] = s_{23}c_{23}s_{12}c_{12}s_{13}c_{13}^2 \sin \delta_{CP}, \quad (17)$$

$$m_{ee} = |m_1 \cos^2 \theta_{12} \cos^2 \theta_{13} + m_2 \sin^2 \theta_{12} \cos^2 \theta_{13} e^{i\alpha_{21}} + m_3 \sin^2 \theta_{13} e^{i(\alpha_{31} - 2\delta_{CP})}|. \quad (18)$$

Tremendous experimental efforts are going on to measure the effective Majorana mass parameter  $m_{ee}$  and it is expected to be measured by KamLAND-Zen experiment in the near future [77].

### III. NUMERICAL ANALYSIS

For numerical analysis, we use the neutrino oscillation parameters from the global-fit results [78–80] obtained from various experiments, as given in Table II. The numerical diagonalization of the light neutrino mass matrix given in eqn.(16), is done through

Oscillation Parameters	Best fit $\pm 1\sigma$	$2\sigma$ range	$3\sigma$ range
$\Delta m_{21}^2 [10^{-5} \text{ eV}^2]$	$7.56 \pm 0.19$	7.20–7.95	7.05–8.14
$ \Delta m_{31}^2  [10^{-3} \text{ eV}^2]$ (NO)	$2.55 \pm 0.04$	2.47–2.63	2.43–2.67
$\sin^2 \theta_{12} / 10^{-1}$	$3.21^{+0.18}_{-0.16}$	2.89–3.59	2.73–3.79
$\sin^2 \theta_{23} / 10^{-1}$ (NO)	$4.30^{+0.20}_{-0.18}$ $5.98^{+0.17}_{-0.15}$	3.98–4.78 & 5.60–6.17 4.09–4.42 & 5.61–6.27	3.84–6.35 3.89–4.88 & 5.22–6.41
$\sin^2 \theta_{13} / 10^{-2}$ (NO)	$2.155^{+0.090}_{-0.075}$	1.98 – 2.31	2.04 – 2.43
$\delta_{CP} / \pi$ (NO)	$1.08^{+0.13}_{-0.12}$	0.84 – 1.42	0.71 – 1.99

TABLE II: The global-fit values of the oscillation parameters alongwith their  $1\sigma$ ,  $2\sigma$  and  $3\sigma$  ranges [78–80].

$U_\nu^\dagger \mathcal{M} U_\nu = \text{diag}(m_1^2, m_2^2, m_3^2)$ , where  $\mathcal{M} = m_\nu m_\nu^\dagger$  and  $U_\nu$  is an unitary matrix. Thus, the lepton mixing matrix is given as  $U = U_i^\dagger U_\nu$ , from which the mixing angles can be excerpted using the standard relations:

$$\sin^2 \theta_{13} = |U_{13}|^2, \quad \sin^2 \theta_{12} = \frac{|U_{12}|^2}{1 - |U_{13}|^2}, \quad \sin^2 \theta_{23} = \frac{|U_{23}|^2}{1 - |U_{13}|^2}. \quad (19)$$

To fit to the current neutrino oscillation data, we use the following ranges for the model parameters:

$$\text{Re}[\tau] \in [0, 0.5], \quad \text{Im}[\tau] \in [1, 3], \quad G_D \in [10^{-7}, 10^{-6}], \quad G_{LS} \in [10^{-4}, 10^{-3}] \quad v_\zeta \in [10, 100] \text{ TeV}, \\ B_{MRS} \in [10^{-3}, 10^{-2}], \quad \Lambda \in [10^4, 10^5] \text{ TeV}. \quad (20)$$

The input parameters are varied randomly in the ranges as provided in Eqn. (20) and constrained by imposing the  $3\sigma$  bounds on neutrino oscillation data, i.e., the solar and atmospheric mass squared differences and the mixing angles as presented in Table II, as well as the sum of active neutrino masses  $\Sigma m_i < 0.12 \text{ eV}$  [81, 82]. The typical range of the modulus  $\tau$  is found to be:  $0 \lesssim \text{Re}[\tau] \lesssim 0.5$  and  $1 \lesssim \text{Im}[\tau] \lesssim 3$  for normal ordered neutrino masses. In Fig. 1, we show the variation of the sum of active neutrino masses ( $\Sigma m_i$ ) with the reactor mixing angle  $\sin^2 \theta_{13}$  in the left panel, while the right panel demonstrates  $\Sigma m_i$  versus  $\sin^2 \theta_{12}$  and  $\sin^2 \theta_{23}$ . From these figures, it can be observed that the model predictions for the sum of neutrino masses as  $\Sigma 0.058 \text{ eV} \leq m_i \leq 0.062 \text{ eV}$  for the allowed  $3\sigma$  ranges of the mixing angles.

The variation of the effective neutrinoless double beta decay mass parameter  $m_{ee}$  with  $\Sigma m_i$  is displayed in Fig. 2, from which the upper limit on  $m_{ee}$  is found to be  $0.025 \text{ eV}$  satisfying KamLAND-Zen bound. Further, we display the variation of  $\delta_{CP}$  and  $J_{CP}$  in the left and right panel of Fig. 3 respectively, where  $100^\circ \leq \delta_{CP} \leq 250^\circ$  and  $|J_{CP}| \leq 0.004$ .

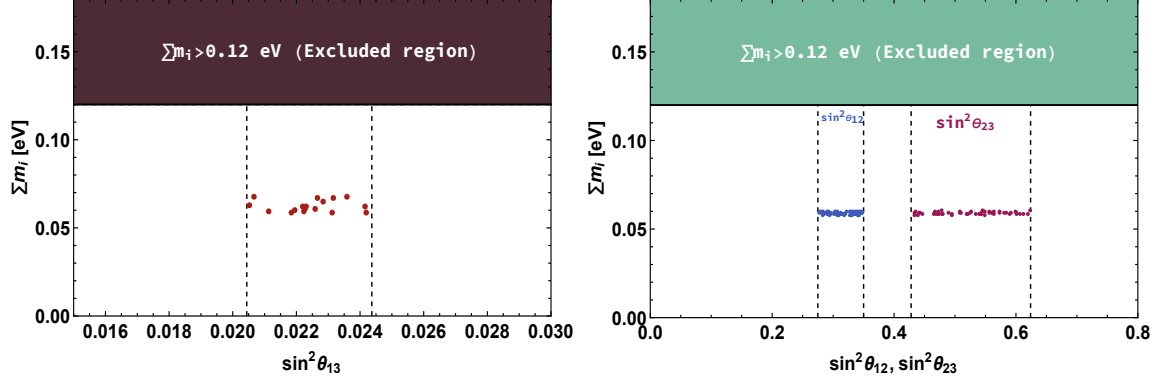


FIG. 1: Left (Right) panel displays the correlation between  $\sin^2 \theta_{13}$  ( $\sin^2 \theta_{12}$  &  $\sin^2 \theta_{23}$ ) with the sum of active neutrino masses. The vertical lines represent the  $3\sigma$  allowed ranges of the mixing angles.

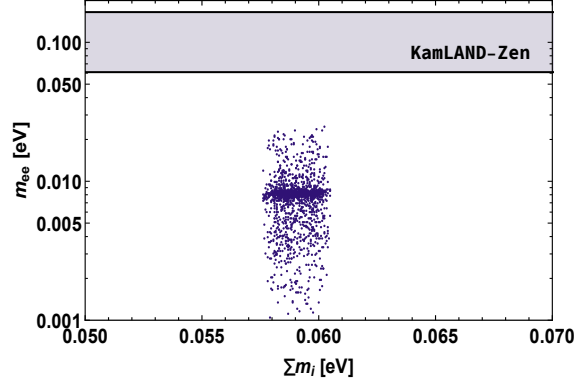


FIG. 2: Correlation plot between the effective neutrino mass  $m_{ee}$  of neutrinoless double beta decay and the sum of active neutrino masses.

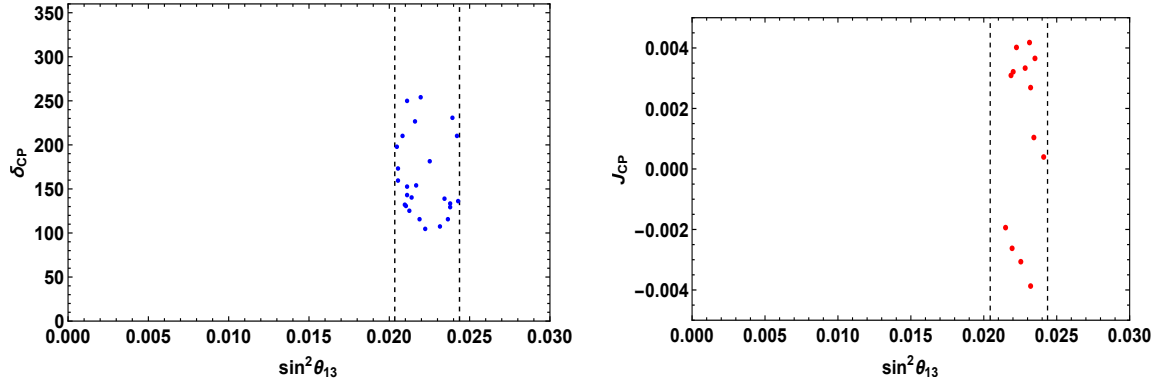


FIG. 3: Left (right) panel shows the plot of  $\delta_{CP}$  ( $J_{CP}$ ) with  $\sin^2 \theta_{13}$  within its  $3\sigma$  bound.

## Comment on non-unitarity of leptonic mixing matrix

Here, we present a brief discussion on the non-unitarity of neutrino mixing matrix  $U'_{\text{PMNS}}$  in the context of the present model. Due to the mixing between the light and heavy fermions, there will be small deviation from unitarity of the leptonic mixing matrix, which can be expressed as following [83]

$$U'_{\text{PMNS}} \equiv \left( 1 - \frac{1}{2} F F^\dagger \right) U_{\text{PMNS}}. \quad (21)$$

Here,  $U_{\text{PMNS}}$  denotes the leptonic mixing matrix that diagonalises the light neutrino mass matrix and  $F$  represents the mixing of active neutrinos with the heavy fermions, approximated as  $F \equiv (M_{NS}^T)^{-1} M_D \approx \frac{g_D v}{\alpha_{RS} v_\zeta}$ , and is a hermitian matrix. The local constraints on the non-unitarity parameters [84–86], are obtained through various experimental results on electroweak parameters, e.g., the mass of  $W$  boson ( $M_W$ ), the Weinberg mixing angle ( $\theta_W$ ), several ratios of fermionic  $Z$  boson decays as well as its invisible decay, bounds from CKM unitarity, and lepton flavor violations. In the context of the present model, we presume the following approximated normalized order for the Dirac, pseudo-Dirac and heavy fermion masses for correctly generating the observed solar and atmospheric mass-squared differences as well as the sum of active neutrino masses of desired order as

$$\left( \frac{m_\nu}{0.1 \text{ eV}} \right) \approx \left( \frac{M_D}{10^{-3} \text{ GeV}} \right) \left( \frac{M_{RS}}{10^3 \text{ GeV}} \right)^{-1} \left( \frac{M_{LS}}{10^{-4} \text{ GeV}} \right). \quad (22)$$

With these chosen order masses, we obtain an approximated non-unitary mixing for the present model as

$$|F F^\dagger| \leq \begin{bmatrix} 4.5 \times 10^{-13} & 2.3 \times 10^{-13} & 6.2 \times 10^{-13} \\ 2.3 \times 10^{-13} & 2.08 \times 10^{-12} & 4.5 \times 10^{-12} \\ 6.2 \times 10^{-13} & 4.5 \times 10^{-12} & 5.6 \times 10^{-12} \end{bmatrix}. \quad (23)$$

As the mixing between the active light and heavy fermions in our model is quite small, it leads to a negligible contribution for the non-unitarity.

## IV. LEPTOGENESIS

The present universe is clearly seen to be baryon dominated, with the ratio of the measured over-abundance of baryons over anti-baryons to the entropy density is found to be

$$Y_B = (8.56 \pm 0.22) \times 10^{-11}. \quad (24)$$

If the universe had started from an initially symmetric state of baryons and antibaryons, following three conditions have to be fulfilled for generating a non-zero baryon asymmetry. According to Sakharov [87], these three criteria are: Baryon number violation, C and CP

violation and departure from equilibrium during the evolution of the universe. Though the SM assures all these criteria for an expanding Universe akin ours, the extent of CP violation found in the SM is quite small to accommodate the observed baryon asymmetry of the universe. Therefore, additional sources of CP violation are absolutely essential for explaining this asymmetry. The most common new sources of CP violation possibly could arise in the lepton sector, which is however, not yet firmly established. experimentally. Leptogenesis is the phenomenon that furnishes a minimal set up to correlate the CP violation in the lepton sector to the observed baryon asymmetry, as well as imposes indirect constraints on the CP phases from the requirement that it would yield the correct baryon asymmetry. It is seen that the scale of CP-asymmetry generated from the heavy neutral fermion decays can come down to as low as TeV [88–91] due to resonant enhancement. However, the present scenario is realized by involving six heavy states, which comprises three pairs of heavy neutrinos with doubly degenerate masses Eq.(14). Nevertheless, introduction of a higher dimensional mass terms for the Majorana fermions ( $N_R$ ) can be made through the following superpotential

$$\mathcal{W}_{M_R} = -G_R \left[ \sum_{i=1}^2 Y_{\mathbf{5},i}^{(4)} N_R^c N_R^c \right] \frac{\zeta'^2}{\Lambda}, \quad (25)$$

which gives rise to a petty mass splitting between the heavy neutral fermions, and hence provides an enhancement in the CP asymmetry for generating the required lepton asymmetry [92, 93]. Thus, from (25) one can construct the Majorana mass matrix for the right-handed neutrinos  $N_R$  as

$$M_R = \frac{G_R v_\zeta^2}{2\Lambda\sqrt{30}} \begin{bmatrix} 2 \left( \sum_{i=1}^2 Y_{\mathbf{5},i}^{(4)} \right)_1 & -\sqrt{3} \left( \sum_{i=1}^2 Y_{\mathbf{5},i}^{(4)} \right)_4 & -\sqrt{3} \left( \sum_{i=1}^2 Y_{\mathbf{5},i}^{(4)} \right)_3 \\ -\sqrt{3} \left( \sum_{i=1}^2 Y_{\mathbf{5},i}^{(4)} \right)_4 & \sqrt{6} \left( \sum_{i=1}^2 Y_{\mathbf{5},i}^{(4)} \right)_2 & - \left( \sum_{i=1}^2 Y_{\mathbf{5},i}^{(4)} \right)_1 \\ -\sqrt{3} \left( \sum_{i=1}^2 Y_{\mathbf{5},i}^{(4)} \right)_3 & - \left( \sum_{i=1}^2 Y_{\mathbf{5},i}^{(4)} \right)_1 & \sqrt{6} \left( \sum_{i=1}^2 Y_{\mathbf{5},i}^{(4)} \right)_5 \end{bmatrix}_{LR}. \quad (26)$$

The coupling  $G_R$  is considered as extremely small to preserve the linear seesaw texture of the neutrino mass matrix (15), i.e.,  $M_D, M_{LS} \gg M_R$  and hence, inclusion of such additional term does not alter the previous results. However, this added term generates a small mass splitting. Hence, the  $2 \times 2$  submatrix of eqn. (15) in the basis of  $(N_R, S_L)$ , becomes

$$M = \begin{pmatrix} M_R & M_{RS} \\ M_{RS}^T & 0 \end{pmatrix}, \quad (27)$$

which can be block diagonalized by the unitary matrix  $\frac{1}{\sqrt{2}} \begin{pmatrix} I & -I \\ I & I \end{pmatrix}$  as

$$M' = \begin{pmatrix} M_{RS} + \frac{M_R}{2} & -\frac{M_R}{2} \\ -\frac{M_R}{2} & -M_{RS} + \frac{M_R}{2} \end{pmatrix} \approx \begin{pmatrix} M_{RS} + \frac{M_R}{2} & 0 \\ 0 & -M_{RS} + \frac{M_R}{2} \end{pmatrix}. \quad (28)$$

Thus, one can express the mass eigenstates ( $N^\pm$ ) in terms of the flavor states ( $N_R, S_L$ ) as

$$\begin{pmatrix} S_{Li} \\ N_{Ri} \end{pmatrix} = \begin{pmatrix} \cos \theta & -\sin \theta \\ \sin \theta & \cos \theta \end{pmatrix} \begin{pmatrix} N_i^+ \\ N_i^- \end{pmatrix}. \quad (29)$$

Assuming the mixing to be maximal, one can have

$$N_{Ri} = \frac{(N_i^+ + N_i^-)}{\sqrt{2}}, \quad S_{Li} = \frac{(N_i^+ - N_i^-)}{\sqrt{2}}. \quad (30)$$

Hence, the interaction superpotential (8) can be manifested in terms of the new basis. The mass eigenvalues of the new states  $N^+$  and  $N^-$  can be obtained by diagonalizing the block-diagonal form of the heavy-fermion masses and are found as  $\frac{M_R}{2} + M_{RS}$  and  $\frac{M_R}{2} - M_{RS}$  (28).

The Dirac (10) and pseudo-Dirac (11) terms are now modified as

$$\mathcal{W}_D = G_D L_L H_u \left[ Y_5^{(2)} \left( \frac{(N_i^+ + N_i^-)}{\sqrt{2}} \right) \right], \quad (31)$$

and

$$\mathcal{W}_{LS} = G_{LS} L_L H_u \left[ \sum_2^{i=1} Y_{4,i}^{(6)} \left( \frac{(N_i^+ - N_i^-)}{\sqrt{2}} \right) \right] \frac{\zeta}{\Lambda}. \quad (32)$$

Thus, one can symbolically express the block-diagonal matrix for the heavy fermions (28) as

$$M_{RS} \pm \frac{M_R}{2} = \frac{v_\zeta}{\sqrt{60}} B_{M_{RS}} \begin{bmatrix} 2a & d & e \\ d & b & f \\ e & f & c \end{bmatrix}_{LR} \pm \frac{G_R v_\zeta^2}{2\Lambda\sqrt{30}} \begin{bmatrix} 2a' & d' & e' \\ d' & b' & f' \\ e' & f' & c' \end{bmatrix}_{LR}, \quad (33)$$

where, the different matrix elements are defined as

$$a(a') = \left( \sum_{i=1}^2 Y_{5,i}^{6(4)} \right)_1, \quad b(b') = \sqrt{6} \left( \sum_{i=1}^2 Y_{5,i}^{6(4)} \right)_2, \quad c(c') = \sqrt{6} \left( \sum_{i=1}^2 Y_{5,i}^{6(4)} \right)_5. \quad (34)$$

$$d(d') = -\sqrt{3} \left( \sum_{i=1}^2 Y_{5,i}^{6(4)} \right)_4, \quad e(e') = -\sqrt{3} \left( \sum_{i=1}^2 Y_{5,i}^{6(4)} \right)_3, \quad f(f') = -a(a'). \quad (35)$$

One can obtain the diagonalized mass matrix from (33) through rotation to the mass eigen-basis as:  $(M^\pm)_{\text{diag}} = U_{\text{TBM}} U_R \left( M_{RS} \pm \frac{M_R}{2} \right) U_R^T U_{\text{TBM}}^T$ , and thus three sets of nearly degenerate mass states can be obtained upon diagonalization. We further presume that the lightest pair among them with mass in the TeV range, contribute predominantly to the CP asymmetry. The small mass difference between the lightest pair demonstrates that the CP asymmetry generated from the one-loop self energy contribution of heavy particle decay dominates over the vertex part. Thus, the CP asymmetry can be expressed as [88, 94]

$$\epsilon_{N_i^-} \approx \frac{1}{32\pi^2 A_{N_i^-}} \text{Im} \left[ \left( \frac{\tilde{M}_D}{v} - \frac{\tilde{M}_{LS}}{v} \right)^\dagger \left( \frac{\tilde{M}_D}{v} + \frac{\tilde{M}_{LS}}{v} \right)^2 \left( \frac{\tilde{M}_D}{v} - \frac{\tilde{M}_{LS}}{v} \right)^\dagger \right]_{ii} \frac{r_N}{r_N^2 + 4A_{N_i^-}^2}, \quad (36)$$

where  $\tilde{M}_{D(LS)} = M_{D(LS)} U_{\text{TBM}} U_R$ ,  $\Delta M = M_i^+ - M_i^- \approx M_R$  and the parameters  $r_N$  and  $A_{N^-}$  are given as

$$r_N = \frac{(M_i^+)^2 - (M_i^-)^2}{M_i^+ M_i^-} = \frac{\Delta M (M_i^+ + M_i^-)}{M_i^+ M_i^-},$$

$$A_{N^-} \approx \frac{1}{16\pi} \left[ \left( \frac{\tilde{M}_D}{v} - \frac{\tilde{M}_{LS}}{v} \right) \left( \frac{\tilde{M}_D}{v} + \frac{\tilde{M}_{LS}}{v} \right) \right]_{ii}. \quad (37)$$

In Fig. 4, we depict the behavior of CP asymmetry with  $r_N$ , which satisfies both neutrino oscillation data and the CP asymmetry required for leptogenesis [95, 96], which will be discussed in the next subsection.

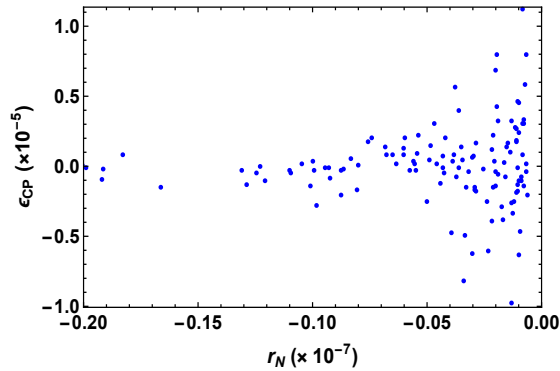


FIG. 4: Correlation plot demonstrating the dependence of CP asymmetry with the parameter  $r_N$ .

### A. Boltzmann Equations

Boltzmann equations are invoked to solve for the lepton asymmetry. It should be reiterated that, the Sakharov criteria [87] require the decay of the parent heavy fermion which ought to be out of equilibrium for generating the lepton asymmetry. In order to implement this condition, one has to confront the Hubble rate to the decay rate as

$$K_{N_i^-} = \frac{\Gamma_{N_i^-}}{H(T = M_i^-)}. \quad (38)$$

Here,  $H = \frac{1.67\sqrt{g_*} T^2}{M_{\text{Pl}}}$  is the Hubble expansion rate, with  $g_* = 106.75$  is the number of relativistic degrees of freedom in the thermal bath and  $M_{\text{Pl}} = 1.22 \times 10^{19}$  GeV is the Planck mass. Coupling strength becomes the deciding factor which guarantees inverse decay does not come into thermal equilibrium. For instance, if the strength is below  $10^{-7}$  it gives  $K_{N^-} \sim 1$ . The Boltzmann equations associated with evolution of the number densities of right-handed fermion field and lepton, articulated in terms of yield parameter (ratio of number density to entropy density) are

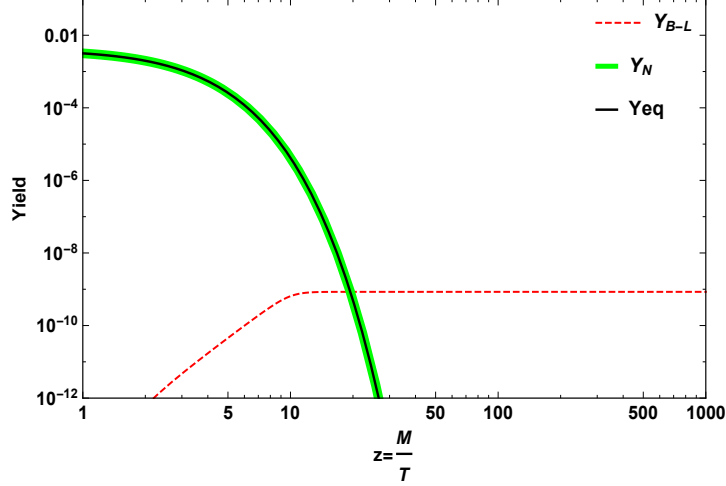


FIG. 5: Evolution of the yield parameters  $Y_N$  and  $Y_{\mathcal{L}}$  as a function of  $z = M_{N^-}/T$ .

given by [96–100]

$$\begin{aligned} \frac{dY_{N^-}}{dz} &= -\frac{z}{sH(M_{N^-})} \left[ \left( \frac{Y_{N^-}}{Y_{N^-}^{\text{eq}}} - 1 \right) \gamma_D + \left( \left( \frac{Y_{N^-}}{Y_{N^-}^{\text{eq}}} \right)^2 - 1 \right) \gamma_S \right], \\ \frac{dY_{B-L}}{dz} &= -\frac{z}{sH(M_{N^-})} \left[ 2 \frac{Y_{B-L}}{Y_{\ell}^{\text{eq}}} \gamma_{Ns} - \epsilon_{N^-} \left( \frac{Y_{N^-}}{Y_{N^-}^{\text{eq}}} - 1 \right) \gamma_D \right], \end{aligned} \quad (39)$$

where  $s$  denotes the entropy density,  $z = M_i^-/T$ ,  $Y_{\mathcal{L}} = Y_{\ell} - Y_{\bar{\ell}}$  and the equilibrium number densities are given as [95]

$$Y_{N^-}^{\text{eq}} = \frac{135g_{N^-}}{16\pi^4g_{\star}} z^2 K_2(z), \quad Y_{\ell}^{\text{eq}} = \frac{3}{4} \frac{45\zeta(3)g_{\ell}}{2\pi^4g_{\star}}. \quad (40)$$

Here,  $K_{1,2}$  are the modified Bessel functions,  $g_{\ell} = 2$  and  $g_{N^-} = 2$  represent the degrees of freedom of lepton and RH fermions,  $\gamma_D$  is the decay rate and is given as

$$\gamma_D = sY_{N^-}^{\text{eq}} \Gamma_{N^-} \frac{K_1(z)}{K_2(z)}. \quad (41)$$

While  $\gamma_S$  represents the scattering rate of  $N^- N^- \rightarrow \zeta \zeta$  [100] and  $\gamma_{Ns}$  denotes the scattering rate of  $\Delta L = 2$  process. One can keep away the delicacy of the asymmetry being produced even when  $N^-$  is in thermal equilibrium by subtracting the contribution arising from on-shell  $N^-$  exchange:  $(\frac{\gamma_D}{4})$  from the total rate  $\gamma_{Ns}$ , given as  $\gamma_{Ns}^{\text{sub}} = \gamma_{Ns} - \frac{\gamma_D}{4}$  [98]. The solution of Boltzmann eq. (39) is displayed in Fig. 5. For large coupling strength  $Y_{N^-}$  (green-thick curve) almost traces  $Y_{N^-}^{\text{eq}}$  (black-solid curve) and the lepton asymmetry (red-dashed curve) is generated. The obtained lepton asymmetry can be converted to the baryon asymmetry through the process of sphaleron transition, given as [97]

$$Y_B = - \left( \frac{8N_f + 4N_H}{22N_f + 13N_H} \right) Y_{\mathcal{L}}, \quad (42)$$

where  $N_f$  represents the number of fermion generations and  $N_H$  denotes the number of Higgs doublets. The observed baryon asymmetry can be expressed in terms of baryon to photon ratio as

[82]

$$\eta = \frac{\eta_b - \eta_{\bar{b}}}{\eta_\gamma} = 6.08 \times 10^{-10}. \quad (43)$$

The current bound on baryon asymmetry can be procured from the relation  $Y_B = \eta/7.04$  as  $Y_B \sim 8.6 \times 10^{-11}$ . Using the asymptotic value of  $Y_{\mathcal{L}}$  as  $(8.77 \times 10^{-10})$  from Fig. 5, the obtained baryon asymmetry is  $Y_B = -\frac{28}{79} Y_{\mathcal{L}} \sim 10^{-10}$ .

### B. A note on flavor consideration

$\epsilon_{N^-}^e$	$\epsilon_{N^-}^\mu$	$\epsilon_{N^-}^\tau$	$\epsilon_{N^-}$	$\Delta M$ (GeV)
$-1.78 \times 10^{-5}$	$-2.6 \times 10^{-5}$	$-4.15 \times 10^{-5}$	$-8.53 \times 10^{-5}$	$4 \times 10^{-6}$

TABLE III: CP asymmetries and mass splitting obtained from the allowed range of model parameters which satisfy neutrino oscillation data.

In leptogenesis, one flavor approximation is sufficient when ( $T > 10^{12}$  GeV), meaning all the Yukawa interactions are out of equilibrium. But for temperatures  $T \ll 10^8$  GeV, several charged lepton Yukawa couplings come into equilibrium making flavor effects an important consideration for generating the final lepton asymmetry. For temperatures below  $10^6$  GeV, all the Yukawa interactions are in equilibrium and the asymmetry is stored in the individual lepton flavor. The detailed investigation of flavor effects in type-I leptogenesis can be seen in myriad literature [101–106].

The Boltzmann equation for generating the lepton asymmetry in each flavor is [102]

$$\frac{dY_{B-L\alpha}^\alpha}{dz} = -\frac{z}{sH(M_1^-)} \left[ \epsilon_{N^-}^\alpha \left( \frac{Y_{N^-}}{Y_{N^-}^{eq}} - 1 \right) \gamma_D - \left( \frac{\gamma_D^\alpha}{2} \right) \frac{A_{\alpha\alpha} Y_{B-L\alpha}^\alpha}{Y_\ell^{eq}} \right], \quad (44)$$

where,  $\epsilon_{N^-}^\alpha$  i.e. ( $\alpha = e, \mu, \tau$ ) represents the CP asymmetry in each lepton flavor

$$\gamma_D^\alpha = sY_{N^-}^{eq} \Gamma_{N^-}^\alpha \frac{K_1(z)}{K_2(z)}, \quad \gamma_D = \sum_\alpha \gamma_D^\alpha.$$

The matrix  $A$  is given by [103],

$$A = \begin{pmatrix} -\frac{221}{711} & \frac{16}{711} & \frac{16}{711} \\ \frac{16}{711} & -\frac{221}{711} & \frac{16}{711} \\ \frac{16}{711} & \frac{16}{711} & -\frac{221}{711} \end{pmatrix}.$$

From the benchmark considered in Table. III, we estimate the  $B - L$  yield with flavor consideration in the left panel of Fig. 6. It is quite obvious to notice that the enhancement in  $B - L$  asymmetry is obtained in case of flavor consideration (blue line) over the one flavor approximation (red line), as displayed in the right panel. This is because, in one flavor approximation the decay of the heavy fermion to a particular lepton flavor final state can get washed away by the inverse decays of any flavor unlike the flavoured case [104].

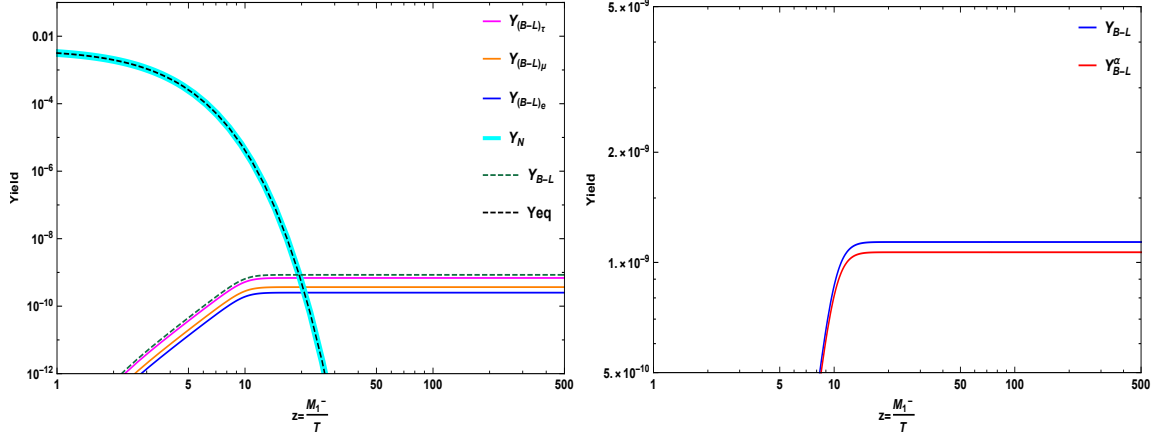


FIG. 6: After including the flavor effects the yield is shown in left panel, whereas, right panel shows the enhancement in the yield due to flavor effects.

## V. SUMMARY AND CONCLUSION

In this work, we have investigated the implications of  $A'_5$  modular symmetry on neutrino phenomenology. The important feature of the modular flavor symmetry is that it reduces the complications of accommodating multiple flavons, which are usually associated with the use of discrete flavor symmetries. In the present model, we consider the SM to be extended by the  $A'_5$  modular symmetry along with a  $U(1)_{B-L}$  local gauge symmetry. It encompasses three right-handed as well as three left-handed heavy fermion fields to explore the neutrino phenomenology within the context of linear seesaw. In addition, it contains a pair of singlet scalars, which play a vital role in spontaneous breaking of  $U(1)_{B-L}$  local symmetry and provide masses to the heavy fermions. The Yukawa couplings are considered to transform non-trivially under modular  $A'_5$  group, which basically replace the role of conventional flavon fields. This in turn, leads to a specific flavor structure for the neutrino mass matrix and helps in exploring the phenomenology of neutrino mixing. We numerically diagonalized the neutrino mass matrix to obtain the allowed regions for the model parameters, compatible with the current  $3\sigma$  limit of oscillation data. Further, our model predicts the CP violating phase  $\delta_{CP}$  to be in the range of  $(100^\circ - 250^\circ)$  and the Jarlskog invariant to be  $\mathcal{O}(10^{-3})$ . The sum of active neutrino masses is found to be in the range  $0.058 \text{ eV} \leq \Sigma m_i \leq 0.062 \text{ eV}$  and the value of effective neutrinoless double beta decay mass parameter  $m_{ee}$  as  $(0.001 - 0.025) \text{ eV}$ , which is quite below the current upper limits from KamLAND-Zen experiment i.e.,  $< (61 - 165) \text{ meV}$ . In addition, the flavor structure of heavy fermions gives rise to three sets of doubly degenerate mass eigenstates and hence, to incorporate leptogenesis, we introduced a higher dimension mass term for the right-handed neutrinos for generating a small mass splitting. We then obtained a non-zero CP asymmetry from the lightest heavy fermion decay where the self energy contribution

is partially enhanced due to the small mass splitting between the two lightest heavy fermions. Utilizing a particular benchmark of model parameters consistent with oscillation data, we tackled coupled Boltzmann equations to get the evolution of lepton asymmetry at TeV scale that emerges to be of the order  $\simeq 10^{-10}$ , which is adequate to explain the present baryon asymmetry of the universe. Besides, we have additionally shed light on the increase in asymmetry due to flavor consideration.

## Acknowledgments

MKB acknowledges DST for its financial help. RM would like acknowledge SERB, Government of India for the support received through grant No. EMR/2017/001448 and University of Hyderabad IoE project grant no. RC1-20-012. We also acknowledge the use of CMSD HPC facility of Univ. of Hyderabad for carrying out the computational work.

## Appendix A: The modular space of $\Gamma(5)$

In order to assert the modular forms which change nontrivially under  $\Gamma'_5 \simeq A'_5$ , it is necessary to first find out the modular space of  $\Gamma(5)$ . Therefore, if  $k$  is an integer i.e. non-negative, the modular space  $M_k[\Gamma(5)]$  bearing weight  $k$  for  $\Gamma(5)$  contains  $5k + 1$  linearly independent modular forms, which act like the basis vectors of the modular space. As stated in Ref. [107], we have

$$M_k[\Gamma(5)] = \bigoplus_{\substack{a+b=5k \\ a,b \geq 0}} \mathbb{C} \frac{\eta(5\tau)^{15k}}{\eta(\tau)^{3k}} \mathfrak{f}_{\frac{1}{5}, \frac{0}{5}}^a(5\tau) \mathfrak{f}_{\frac{2}{5}, \frac{0}{5}}^b(5\tau), \quad (45)$$

represented below is the Dedekind eta function  $\eta(\tau)$

$$\eta(\tau) = q^{1/24} \prod_{n=1}^{\infty} (1 - q^n), \quad (46)$$

where,  $q \equiv e^{2i\pi\tau}$ , and  $\mathfrak{f}_{r_1, r_2}(\tau)$  is the Klein form

$$\mathfrak{f}_{r_1, r_2}(\tau) = q_z^{(r_1-1)/2} (1 - q_z) \times \prod_{n=1}^{\infty} (1 - q^n q_z) (1 - q^n q_z^{-1}) (1 - q^n)^{-2}, \quad (47)$$

where  $(r_1, r_2)$  illustrates a pair of rational numbers in the domain of  $\mathbb{Q}^2 - \mathbb{Z}^2$ ,  $z \equiv \tau r_1 + r_2$  and  $q_z \equiv e^{2i\pi z}$ . Under the transformations of  $S$  and  $T$ , the eta function and the Klein form change as follows

$$\begin{aligned} S: \eta(\tau) &\rightarrow \sqrt{-i\tau} \eta(\tau), \quad \mathfrak{f}_{r_1, r_2}(\tau) \rightarrow -\frac{1}{\tau} \mathfrak{f}_{-r_2, r_1}(\tau), \\ T: \eta(\tau) &\rightarrow e^{i\pi/12} \eta(\tau), \quad \mathfrak{f}_{r_1, r_2}(\tau) \rightarrow \mathfrak{f}_{r_1, r_1+r_2}(\tau). \end{aligned} \quad (48)$$

More information about the properties of the Klein form  $\mathfrak{f}_{r_1, r_2}(\tau)$  can be found in Refs. [107, 108].

## Appendix B: Higher Order Yukawa couplings

All higher order Yukawa couplings are expressed in terms of the elements of  $Y_{\widehat{6}}^{(1)}$  Yukawa coupling expressed as

$$Y_{\widehat{6}}^{(1)} = \begin{bmatrix} Y_1 \\ Y_2 \\ Y_3 \\ Y_4 \\ Y_5 \\ Y_6 \end{bmatrix} = \begin{bmatrix} \widehat{e}_1 - 3\widehat{e}_6 \\ 5\sqrt{2}\widehat{e}_2 \\ 10\widehat{e}_3 \\ 10\widehat{e}_4 \\ 5\sqrt{2}\widehat{e}_5 \\ -3\widehat{e}_1 - \widehat{e}_6 \end{bmatrix}. \quad (49)$$

Below are the modular form of the Yukawa couplings utilized to construct our model and the other couplings seen in the tensor product are expressed in [70]

$$Y_{\mathbf{3}}^{(2)} = \left[ Y_{\widehat{6}}^{(1)} \otimes Y_{\widehat{6}}^{(1)} \right]_{\mathbf{3}_{s,1}} = -3 \begin{bmatrix} \widehat{e}_1^2 - 36\widehat{e}_1\widehat{e}_6 - \widehat{e}_6^2 \\ 5\sqrt{2}\widehat{e}_2(\widehat{e}_1 - 3\widehat{e}_6) \\ 5\sqrt{2}\widehat{e}_5(3\widehat{e}_1 + \widehat{e}_6) \end{bmatrix} = -3 \begin{bmatrix} Y_1^2 - 3Y_1Y_6 - Y_6^2 \\ Y_1Y_2 \\ -Y_5Y_6 \end{bmatrix}, \quad (50)$$

$$Y_{\mathbf{3}}^{(4)} = \left[ Y_{\widehat{6}}^{(1)} \otimes Y_{\widehat{6},2}^{(3)} \right]_{\mathbf{3}_{s,1}} = \frac{\sqrt{3}}{4} \begin{bmatrix} (Y_1^2 + Y_6^2)(7Y_1^2 - 18Y_1Y_6 - 7Y_6^2) \\ Y_2(13Y_1^3 - 3Y_1^2Y_6 - 29Y_1Y_6^2 - 9Y_6^3) \\ -Y_5(9Y_1^3 - 29Y_1^2Y_6 + 3Y_1Y_6^2 + 13Y_6^3) \end{bmatrix}, \quad (51)$$

$$Y_{\mathbf{3},1}^{(6)} = \left[ Y_{\widehat{6}}^{(1)} \otimes Y_{\widehat{2}'}^{(5)} \right]_{\mathbf{3}} = \frac{9\sqrt{2}}{16} (Y_1^2 - 4Y_1Y_6 - Y_6^2) \begin{bmatrix} (Y_1 - 3Y_6)(3Y_1 + Y_6)(3Y_1^2 - 2Y_1Y_6 - 3Y_6^2) \\ 2Y_2(2Y_1^3 - 9Y_1Y_6^2 - 3Y_6^3) \\ 2Y_5(3Y_1^3 - 9Y_1^2Y_6 + 2Y_6^3) \end{bmatrix}, \quad (52)$$

$$Y_{\mathbf{3},2}^{(6)} = \left[ Y_{\widehat{6}}^{(1)} \otimes Y_{\widehat{6},1}^{(5)} \right]_{\mathbf{3}_{s,1}} = 3\sqrt{2} (Y_1^4 - 3Y_1^3Y_6 - Y_1^2Y_6^2 + 3Y_1Y_6^3 + Y_6^4) \begin{bmatrix} Y_1^2 - 3Y_1Y_6 - Y_6^2 \\ Y_1Y_2 \\ -Y_5Y_6 \end{bmatrix}, \quad (53)$$

$$Y_{\mathbf{4},1}^{(6)} = \left[ Y_{\widehat{6}}^{(1)} \otimes Y_{\widehat{2}}^{(5)} \right]_{\mathbf{4}} = -\frac{3}{4} (Y_1^2 - 4Y_1Y_6 - Y_6^2)^2 \begin{bmatrix} -\sqrt{2}Y_2(3Y_1 + Y_6) \\ Y_3(Y_1 + Y_6) \\ Y_4(Y_1 - Y_6) \\ \sqrt{2}Y_5(Y_1 - 3Y_6) \end{bmatrix}, \quad (54)$$

$$Y_{\mathbf{4},2}^{(6)} = \left[ Y_{\widehat{6}}^{(1)} \otimes Y_{\widehat{2}'}^{(5)} \right]_{\mathbf{4}} = -\frac{\sqrt{6}}{8} (Y_1^2 - 4Y_1Y_6 - Y_6^2) \begin{bmatrix} \sqrt{2}Y_2(Y_1^3 + 11Y_1^2Y_6 + 19Y_1Y_6^2 + 5Y_6^3) \\ Y_3(13Y_1^3 - 31Y_1^2Y_6 - 17Y_1Y_6^2 - Y_6^3) \\ Y_4(Y_1^3 - 17Y_1^2Y_6 + 31Y_1Y_6^2 + 13Y_6^3) \\ \sqrt{2}Y_5(5Y_1^3 - 19Y_1^2Y_6 + 11Y_1Y_6^2 - Y_6^3) \end{bmatrix} \quad (55)$$

$$Y_5^{(2)} = \left[ Y_{\widehat{\mathbf{6}}}^{(1)} \otimes Y_{\widehat{\mathbf{6}}}^{(1)} \right]_{\mathbf{5}_s} = 5 \begin{bmatrix} \sqrt{2} [\widehat{e}_1^2 + \widehat{e}_6^2] \\ -2\sqrt{3} \widehat{e}_2 (\widehat{e}_1 + 7\widehat{e}_6) \\ 2\sqrt{3} \widehat{e}_3 (4\widehat{e}_6 - 3\widehat{e}_1) \\ -2\sqrt{3} \widehat{e}_4 (4\widehat{e}_1 + 3\widehat{e}_6) \\ 2\sqrt{3} \widehat{e}_5 (\widehat{e}_6 - 7\widehat{e}_1) \end{bmatrix} = \frac{1}{2} \begin{bmatrix} \sqrt{2} (Y_1^2 + Y_6^2) \\ 2\sqrt{6} Y_2 (2Y_1 + Y_6) \\ \sqrt{3} Y_3 (Y_6 - 3Y_1) \\ \sqrt{3} Y_4 (Y_1 + 3Y_6) \\ 2\sqrt{6} Y_5 (2Y_6 - Y_1) \end{bmatrix}. \quad (56)$$

$$Y_{\mathbf{5},1}^{(4)} = \left[ Y_{\widehat{\mathbf{6}}}^{(1)} \otimes Y_{\widehat{\mathbf{4}}}^{(3)} \right]_{\mathbf{5},2} = -\frac{3\sqrt{30}}{10} (Y_1^2 - 4Y_1 Y_6 - Y_6^2) \begin{bmatrix} \sqrt{3} (Y_1 - 3Y_6) (3Y_1 + Y_6) \\ -Y_2 (5Y_1 + Y_6) \\ \sqrt{2} Y_3 (Y_1 - Y_6) \\ \sqrt{2} Y_4 (Y_1 + Y_6) \\ -Y_5 (Y_1 - 5Y_6) \end{bmatrix}, \quad (57)$$

$$Y_{\mathbf{5},2}^{(4)} = \left[ Y_{\widehat{\mathbf{6}}}^{(1)} \otimes Y_{\widehat{\mathbf{6},2}}^{(3)} \right]_{\mathbf{5}_{a,1}} = \frac{1}{4} \begin{bmatrix} 11Y_1^4 - 60Y_1^3 Y_6 + 58Y_1^2 Y_6^2 + 60Y_1 Y_6^3 + 11Y_6^4 \\ \sqrt{3} Y_2 (Y_1 + Y_6) (Y_1^2 + 8Y_1 Y_6 + 3Y_6^2) \\ -\sqrt{6} Y_3 (Y_1^3 + 3Y_1^2 Y_6 - 9Y_1 Y_6^2 - 3Y_6^3) \\ \sqrt{6} Y_4 (3Y_1^3 - 9Y_1^2 Y_6 - 3Y_1 Y_6^2 + Y_6^3) \\ -\sqrt{3} Y_5 (Y_1 - Y_6) (3Y_1^2 - 8Y_1 Y_6 + Y_6^2) \end{bmatrix}. \quad (58)$$

$$Y_{\mathbf{5},1}^{(6)} = \left[ Y_{\widehat{\mathbf{6}}}^{(1)} \otimes Y_{\widehat{\mathbf{4}}}^{(5)} \right]_{\mathbf{5},2} = \frac{\sqrt{10}}{8} (Y_1^2 - 4Y_1 Y_6 - Y_6^2) \begin{bmatrix} \sqrt{3} (Y_1 - 3Y_6) (3Y_1 + Y_6) (Y_1^2 + Y_6^2) \\ -2Y_2 (2Y_1 + Y_6) (2Y_1^2 - 3Y_1 Y_6 - Y_6^2) \\ \sqrt{2} Y_3 (Y_1^3 + 2Y_1^2 Y_6 - 11Y_1 Y_6^2 - 4Y_6^3) \\ \sqrt{2} Y_4 (4Y_1^3 - 11Y_1^2 Y_6 - 2Y_1 Y_6^2 + Y_6^3) \\ 2Y_5 (Y_1 - 2Y_6) (Y_1^2 - 3Y_1 Y_6 - 2Y_6^2) \end{bmatrix} \quad (59)$$

$$Y_{\mathbf{5},2}^{(6)} = \left[ Y_{\widehat{\mathbf{6}}}^{(1)} \otimes Y_{\widehat{\mathbf{6},1}}^{(5)} \right]_{\mathbf{5}_s} = -\frac{1}{\sqrt{2}} (Y_1^4 - 3Y_1^3 Y_6 - Y_1^2 Y_6^2 + 3Y_1 Y_6^3 + Y_6^4) \begin{bmatrix} \sqrt{2} (Y_1^2 + Y_6^2) \\ 2\sqrt{6} Y_2 (2Y_1 + Y_6) \\ -\sqrt{3} Y_3 (3Y_1 - Y_6) \\ \sqrt{3} Y_4 (Y_1 + 3Y_6) \\ -2\sqrt{6} Y_5 (Y_1 - 2Y_6) \end{bmatrix} \quad (60)$$

## Appendix A: $A_5'$ Modular Symmetry Product Rule

In this Appendix, we summarize the decomposition rules of the Kronecker products of any two nontrivial irreducible representations of  $A_5'$ , namely,

$$\begin{aligned}
\mathbf{3} \otimes \mathbf{3} &= \mathbf{1}_s \oplus \mathbf{3}_a \oplus \mathbf{5}_s & \mathbf{3}' \otimes \mathbf{3}' &= \mathbf{1}_s \oplus \mathbf{3}'_a \oplus \mathbf{5}_s & \mathbf{3} \otimes \mathbf{3}' &= \mathbf{4} \oplus \mathbf{5} \\
\left\{ \begin{array}{l} \mathbf{1}_s : \frac{\sqrt{3}}{3} (\varrho_1 \vartheta_1 + \varrho_2 \vartheta_3 + \varrho_3 \vartheta_2) \\ \mathbf{3}_a : \frac{\sqrt{2}}{2} \begin{pmatrix} \varrho_2 \vartheta_3 - \varrho_3 \vartheta_2 \\ \varrho_1 \vartheta_2 - \varrho_2 \vartheta_1 \\ \varrho_3 \vartheta_1 - \varrho_1 \vartheta_3 \end{pmatrix} \\ \mathbf{5}_s : \frac{\sqrt{6}}{6} \begin{pmatrix} 2\varrho_1 \vartheta_1 - \varrho_2 \vartheta_3 - \varrho_3 \vartheta_2 \\ -\sqrt{3} \varrho_1 \vartheta_2 - \sqrt{3} \varrho_2 \vartheta_1 \\ \sqrt{6} \varrho_2 \vartheta_2 \\ \sqrt{6} \varrho_3 \vartheta_3 \\ -\sqrt{3} (\varrho_1 \vartheta_3 + \varrho_3 \vartheta_1) \end{pmatrix} \end{array} \right. & \left\{ \begin{array}{l} \mathbf{1}_s : \frac{\sqrt{3}}{3} (\varrho_1 \vartheta_1 + \varrho_2 \vartheta_3 + \varrho_3 \vartheta_2) \\ \mathbf{3}'_a : \frac{\sqrt{2}}{2} \begin{pmatrix} \varrho_2 \vartheta_3 - \varrho_3 \vartheta_2 \\ \varrho_1 \vartheta_2 - \varrho_2 \vartheta_1 \\ \varrho_3 \vartheta_1 - \varrho_1 \vartheta_3 \end{pmatrix} \\ \mathbf{5}_s : \frac{\sqrt{6}}{6} \begin{pmatrix} 2\varrho_1 \vartheta_1 - \varrho_2 \vartheta_3 - \varrho_3 \vartheta_2 \\ \sqrt{6} \varrho_3 \vartheta_3 \\ -\sqrt{3} (\varrho_1 \vartheta_2 + \varrho_2 \vartheta_1) \\ -\sqrt{3} (\varrho_1 \vartheta_3 + \varrho_3 \vartheta_1) \\ \sqrt{6} \varrho_2 \vartheta_2 \end{pmatrix} \end{array} \right. & \left\{ \begin{array}{l} \mathbf{4} : \frac{\sqrt{3}}{3} \begin{pmatrix} \sqrt{2} \varrho_2 \vartheta_1 + \varrho_3 \vartheta_2 \\ -\sqrt{2} \varrho_1 \vartheta_2 - \varrho_3 \vartheta_3 \\ -\sqrt{2} \varrho_1 \vartheta_3 - \varrho_2 \vartheta_2 \\ \sqrt{2} \varrho_3 \vartheta_1 + \varrho_2 \vartheta_3 \end{pmatrix} \\ \mathbf{5} : \frac{\sqrt{3}}{3} \begin{pmatrix} \sqrt{3} \varrho_1 \vartheta_1 \\ \varrho_2 \vartheta_1 - \sqrt{2} \varrho_3 \vartheta_2 \\ \varrho_1 \vartheta_2 - \sqrt{2} \varrho_3 \vartheta_3 \\ \varrho_1 \vartheta_3 - \sqrt{2} \varrho_2 \vartheta_2 \\ \varrho_3 \vartheta_1 - \sqrt{2} \varrho_2 \vartheta_3 \end{pmatrix} \end{array} \right.
\end{aligned}$$

$$\begin{aligned}
\mathbf{4} \otimes \mathbf{4} &= \mathbf{1}_s \oplus \mathbf{3}_a \oplus \mathbf{3}'_a \oplus \mathbf{4}_s \oplus \mathbf{5}_s & \widehat{\mathbf{4}} \otimes \widehat{\mathbf{4}} &= \mathbf{1}_a \oplus \mathbf{3}_s \oplus \mathbf{3}'_s \oplus \mathbf{4}_s \oplus \mathbf{5}_s \\
\left\{ \begin{array}{l} \mathbf{1}_s : \frac{1}{2} (\varrho_1 \vartheta_4 + \varrho_2 \vartheta_3 + \varrho_3 \vartheta_2 + \varrho_4 \vartheta_1) \\ \mathbf{3}_a : \frac{1}{2} \begin{pmatrix} -\varrho_1 \vartheta_4 + \varrho_2 \vartheta_3 - \varrho_3 \vartheta_2 + \varrho_4 \vartheta_1 \\ \sqrt{2} (\varrho_2 \vartheta_4 - \varrho_4 \vartheta_2) \\ \sqrt{2} (\varrho_1 \vartheta_3 - \varrho_3 \vartheta_1) \end{pmatrix} \\ \mathbf{3}'_a : \frac{1}{2} \begin{pmatrix} \varrho_1 \vartheta_4 + \varrho_2 \vartheta_3 - \varrho_3 \vartheta_2 - \varrho_4 \vartheta_1 \\ \sqrt{2} (\varrho_3 \vartheta_4 - \varrho_4 \vartheta_3) \\ \sqrt{2} (\varrho_1 \vartheta_2 - \varrho_2 \vartheta_1) \end{pmatrix} \\ \mathbf{4}_s : \frac{\sqrt{3}}{3} \begin{pmatrix} \varrho_2 \vartheta_4 + \varrho_3 \vartheta_3 + \varrho_4 \vartheta_2 \\ \varrho_1 \vartheta_1 + \varrho_3 \vartheta_4 + \varrho_4 \vartheta_3 \\ \varrho_1 \vartheta_2 + \varrho_2 \vartheta_1 + \varrho_4 \vartheta_4 \\ \varrho_1 \vartheta_3 + \varrho_2 \vartheta_2 + \varrho_3 \vartheta_1 \end{pmatrix} \\ \mathbf{5}_s : \frac{\sqrt{3}}{6} \begin{pmatrix} \sqrt{3} (\varrho_1 \vartheta_4 - \varrho_2 \vartheta_3 - \varrho_3 \vartheta_2 + \varrho_4 \vartheta_1) \\ -\sqrt{2} (\varrho_2 \vartheta_4 - 2\varrho_3 \vartheta_3 + \varrho_4 \vartheta_2) \\ -\sqrt{2} (2\varrho_1 \vartheta_1 - \varrho_3 \vartheta_4 - \varrho_4 \vartheta_3) \\ \sqrt{2} (\varrho_1 \vartheta_2 + \varrho_2 \vartheta_1 - 2\varrho_4 \vartheta_4) \\ -\sqrt{2} (\varrho_1 \vartheta_3 - 2\varrho_2 \vartheta_2 + \varrho_3 \vartheta_1) \end{pmatrix} \end{array} \right. & \left\{ \begin{array}{l} \mathbf{1}_a : \frac{1}{2} (\varrho_1 \vartheta_4 + \varrho_2 \vartheta_3 - \varrho_3 \vartheta_2 - \varrho_4 \vartheta_1) \\ \mathbf{3}_s : -\frac{\sqrt{5}}{10} \begin{pmatrix} 3\varrho_1 \vartheta_4 + \varrho_2 \vartheta_3 + \varrho_3 \vartheta_2 + 3\varrho_4 \vartheta_1 \\ \sqrt{2} (\sqrt{3} \varrho_2 \vartheta_4 - 2\varrho_3 \vartheta_3 + \sqrt{3} \varrho_4 \vartheta_2) \\ \sqrt{2} (\sqrt{3} \varrho_1 \vartheta_3 + 2\varrho_2 \vartheta_2 + \sqrt{3} \varrho_3 \vartheta_1) \end{pmatrix} \\ \mathbf{3}'_s : -\frac{\sqrt{5}}{10} \begin{pmatrix} \varrho_1 \vartheta_4 - 3\varrho_2 \vartheta_3 - 3\varrho_3 \vartheta_2 + \varrho_4 \vartheta_1 \\ \sqrt{2} (2\varrho_1 \vartheta_1 - \sqrt{3} \varrho_3 \vartheta_4 - \sqrt{3} \varrho_4 \vartheta_3) \\ \sqrt{2} (\sqrt{3} \varrho_1 \vartheta_2 + \sqrt{3} \varrho_2 \vartheta_1 - 2\varrho_4 \vartheta_4) \end{pmatrix} \\ \mathbf{4}_s : \frac{\sqrt{5}}{5} \begin{pmatrix} \varrho_2 \vartheta_4 + \sqrt{3} \varrho_3 \vartheta_3 + \varrho_4 \vartheta_2 \\ -\sqrt{3} \varrho_1 \vartheta_1 - \varrho_3 \vartheta_4 - \varrho_4 \vartheta_3 \\ -\varrho_1 \vartheta_2 - \varrho_2 \vartheta_1 - \sqrt{3} \varrho_4 \vartheta_4 \\ -\varrho_1 \vartheta_3 + \sqrt{3} \varrho_2 \vartheta_2 - \varrho_3 \vartheta_1 \end{pmatrix} \\ \mathbf{5}_a : \frac{1}{2} \begin{pmatrix} \varrho_1 \vartheta_4 - \varrho_2 \vartheta_3 + \varrho_3 \vartheta_2 - \varrho_4 \vartheta_1 \\ -\sqrt{2} (\varrho_2 \vartheta_4 - \varrho_4 \vartheta_2) \\ -\sqrt{2} (\varrho_3 \vartheta_4 - \varrho_4 \vartheta_3) \\ \sqrt{2} (\varrho_1 \vartheta_2 - \varrho_2 \vartheta_1) \\ -\sqrt{2} (\varrho_1 \vartheta_3 - \varrho_3 \vartheta_1) \end{pmatrix} \end{array} \right.
\end{aligned}$$

$$\mathbf{5} \otimes \mathbf{5} = \mathbf{1}_s \oplus \mathbf{3}_a \oplus \mathbf{3}'_a \oplus \mathbf{4}_s \oplus \mathbf{4}_a \oplus \mathbf{5}_{s,1} \oplus \mathbf{5}_{s,2}$$

$$\left\{ \begin{array}{l} \mathbf{1}_s : \frac{\sqrt{5}}{5} (\varrho_1 \vartheta_1 + \varrho_2 \vartheta_5 + \varrho_3 \vartheta_4 + \varrho_4 \vartheta_3 + \varrho_5 \vartheta_2) \\ \mathbf{3}_a : \frac{\sqrt{10}}{10} \begin{pmatrix} \varrho_2 \vartheta_5 + 2\varrho_3 \vartheta_4 - 2\varrho_4 \vartheta_3 - \varrho_5 \vartheta_2 \\ -\sqrt{3}\varrho_1 \vartheta_2 + \sqrt{3}\varrho_2 \vartheta_1 + \sqrt{2}\varrho_3 \vartheta_5 - \sqrt{2}\varrho_5 \vartheta_3 \\ \sqrt{3}\varrho_1 \vartheta_5 + \sqrt{2}\varrho_2 \vartheta_4 - \sqrt{2}\varrho_4 \vartheta_2 - \sqrt{3}\varrho_5 \vartheta_1 \end{pmatrix} \\ \mathbf{3}'_a : \frac{\sqrt{10}}{10} \begin{pmatrix} 2\varrho_2 \vartheta_5 - \varrho_3 \vartheta_4 + \varrho_4 \vartheta_3 - 2\varrho_5 \vartheta_2 \\ \sqrt{3}\varrho_1 \vartheta_3 - \sqrt{3}\varrho_3 \vartheta_1 + \sqrt{2}\varrho_4 \vartheta_5 - \sqrt{2}\varrho_5 \vartheta_4 \\ -\sqrt{3}\varrho_1 \vartheta_4 + \sqrt{2}\varrho_2 \vartheta_3 - \sqrt{2}\varrho_3 \vartheta_2 + \sqrt{3}\varrho_4 \vartheta_1 \end{pmatrix} \\ \mathbf{4}_s : \frac{\sqrt{30}}{30} \begin{pmatrix} \sqrt{6}\varrho_1 \vartheta_2 + \sqrt{6}\varrho_2 \vartheta_1 - \varrho_3 \vartheta_5 + 4\varrho_4 \vartheta_4 - \varrho_5 \vartheta_3 \\ \sqrt{6}\varrho_1 \vartheta_3 + 4\varrho_2 \vartheta_2 + \sqrt{6}\varrho_3 \vartheta_1 - \varrho_4 \vartheta_5 - \varrho_5 \vartheta_4 \\ \sqrt{6}\varrho_1 \vartheta_4 - \varrho_2 \vartheta_3 - \varrho_3 \vartheta_2 + \sqrt{6}\varrho_4 \vartheta_1 + 4\varrho_5 \vartheta_5 \\ \sqrt{6}\varrho_1 \vartheta_5 - \varrho_2 \vartheta_4 + 4\varrho_3 \vartheta_3 - \varrho_4 \vartheta_2 + \sqrt{6}\varrho_5 \vartheta_1 \end{pmatrix} \\ \mathbf{4}_a : \frac{\sqrt{10}}{10} \begin{pmatrix} \sqrt{2}\varrho_1 \vartheta_2 - \sqrt{2}\varrho_2 \vartheta_1 + \sqrt{3}\varrho_3 \vartheta_5 - \sqrt{3}\varrho_5 \vartheta_3 \\ -\sqrt{2}\varrho_1 \vartheta_3 + \sqrt{2}\varrho_3 \vartheta_1 + \sqrt{3}\varrho_4 \vartheta_5 - \sqrt{3}\varrho_5 \vartheta_4 \\ -\sqrt{2}\varrho_1 \vartheta_4 - \sqrt{3}\varrho_2 \vartheta_3 + \sqrt{3}\varrho_3 \vartheta_2 + \sqrt{2}\varrho_4 \vartheta_1 \\ \sqrt{2}\varrho_1 \vartheta_5 - \sqrt{3}\varrho_2 \vartheta_4 + \sqrt{3}\varrho_4 \vartheta_2 - \sqrt{2}\varrho_5 \vartheta_1 \end{pmatrix} \\ \mathbf{5}_{s,1} : \frac{\sqrt{14}}{14} \begin{pmatrix} 2\varrho_1 \vartheta_1 + \varrho_2 \vartheta_5 - 2\varrho_3 \vartheta_4 - 2\varrho_4 \vartheta_3 + \varrho_5 \vartheta_2 \\ \varrho_1 \vartheta_2 + \varrho_2 \vartheta_1 + \sqrt{6}\varrho_3 \vartheta_5 + \sqrt{6}\varrho_5 \vartheta_3 \\ -2\varrho_1 \vartheta_3 + \sqrt{6}\varrho_2 \vartheta_2 - 2\varrho_3 \vartheta_1 \\ -2\varrho_1 \vartheta_4 - 2\varrho_4 \vartheta_1 + \sqrt{6}\varrho_5 \vartheta_5 \\ \varrho_1 \vartheta_5 + \sqrt{6}\varrho_2 \vartheta_4 + \sqrt{6}\varrho_4 \vartheta_2 + \varrho_5 \vartheta_1 \end{pmatrix} \\ \mathbf{5}_{s,2} : \frac{\sqrt{14}}{14} \begin{pmatrix} 2\varrho_1 \vartheta_1 - 2\varrho_2 \vartheta_5 + \varrho_3 \vartheta_4 + \varrho_4 \vartheta_3 - 2\varrho_5 \vartheta_2 \\ -2\varrho_1 \vartheta_2 - 2\varrho_2 \vartheta_1 + \sqrt{6}\varrho_4 \vartheta_4 \\ \varrho_1 \vartheta_3 + \varrho_3 \vartheta_1 + \sqrt{6}\varrho_4 \vartheta_5 + \sqrt{6}\varrho_5 \vartheta_4 \\ \varrho_1 \vartheta_4 + \sqrt{6}\varrho_2 \vartheta_3 + \sqrt{6}\varrho_3 \vartheta_2 + \varrho_4 \vartheta_1 \\ -2\varrho_1 \vartheta_5 + \sqrt{6}\varrho_3 \vartheta_3 - 2\varrho_5 \vartheta_1 \end{pmatrix} \end{array} \right.$$

- 
- [1] **T2K**, C. Bronner, “*Details of T2K Oscillation Analysis*,” PoS **NuFact2019** (2020) 037.  
[2] **RENO**, M. Y. Pac, “*Recent Results from RENO*,” PoS **NuFact2017** (2018) 038,  
arXiv:1801.04049.

- [3] **Daya Bay**, Z. Yu, “*Recent Results from the Daya Bay Experiment*,” J. Phys. Conf. Ser. **888** (2017) no. 1, 012011.
- [4] **Double Chooz**, H. de Kerret *et al.*, “*Double Chooz  $\theta_{13}$  measurement via total neutron capture detection*,” Nature Phys. **16** (2020) no. 5, 558–564, [arXiv:1901.09445](#).
- [5] P. F. de Salas, D. V. Forero, S. Gariazzo, P. Martínez-Miravé, O. Mena, C. A. Ternes, M. Tórtola, and J. W. F. Valle, “*2020 global reassessment of the neutrino oscillation picture*,” JHEP **02** (2021) 071, [arXiv:2006.11237](#).
- [6] I. Esteban, M. Gonzalez-Garcia, M. Maltoni, T. Schwetz, and A. Zhou, “*The fate of hints: updated global analysis of three-flavor neutrino oscillations*,” JHEP **09** (2020) 178, [arXiv:2007.14792](#).
- [7] R. N. Mohapatra and G. Senjanovic, “*Neutrino Mass and Spontaneous Parity Nonconservation*,” Phys. Rev. Lett. **44** (1980) 912.
- [8] V. Brdar, A. J. Helmboldt, S. Iwamoto, and K. Schmitz, “*Type-I Seesaw as the Common Origin of Neutrino Mass, Baryon Asymmetry, and the Electroweak Scale*,” Phys. Rev. D **100** (2019) 075029, [arXiv:1905.12634](#).
- [9] G. C. Branco, J. T. Penedo, P. M. F. Pereira, M. N. Rebelo, and J. I. Silva-Marcos, “*Type-I Seesaw with eV-Scale Neutrinos*,” JHEP **07** (2020) 164, [arXiv:1912.05875](#).
- [10] S. Bilenky, *Introduction to the physics of massive and mixed neutrinos*, vol. 817. 2010.
- [11] P.-H. Gu, H. Zhang, and S. Zhou, “*A Minimal Type II Seesaw Model*,” Phys. Rev. D **74** (2006) 076002, [arXiv:hep-ph/0606302](#).
- [12] S. Luo and Z.-z. Xing, “*The Minimal Type-II Seesaw Model and Flavor-dependent Leptogenesis*,” Int. J. Mod. Phys. A **23** (2008) 3412–3415, [arXiv:0712.2610](#).
- [13] S. Antusch and S. F. King, “*Type II Leptogenesis and the neutrino mass scale*,” Phys. Lett. B **597** (2004) 199–207, [arXiv:hep-ph/0405093](#).
- [14] W. Rodejohann, “*Type II seesaw mechanism, deviations from bimaximal neutrino mixing and leptogenesis*,” Phys. Rev. D **70** (2004) 073010, [arXiv:hep-ph/0403236](#).
- [15] P.-H. Gu, “*Double type II seesaw mechanism accompanied by Dirac fermionic dark matter*,” Phys. Rev. D **101** (2020) no. 1, 015006, [arXiv:1907.10019](#).
- [16] J. McDonald, N. Sahu, and U. Sarkar, “*Type-II Seesaw at Collider, Lepton Asymmetry and Singlet Scalar Dark Matter*,” JCAP **04** (2008) 037, [arXiv:0711.4820](#).
- [17] Y. Liao, J.-Y. Liu, and G.-Z. Ning, “*Radiative Neutrino Mass in Type III Seesaw Model*,” Phys. Rev. D **79** (2009) 073003, [arXiv:0902.1434](#).
- [18] E. Ma, “*Pathways to naturally small neutrino masses*,” Phys. Rev. Lett. **81** (1998) 1171–1174, [arXiv:hep-ph/9805219](#).
- [19] R. Foot, H. Lew, X. G. He, and G. C. Joshi, “*Seesaw Neutrino Masses Induced by a Triplet of Leptons*,” Z. Phys. C **44** (1989) 441.
- [20] I. Dorsner and P. Fileviez Perez, “*Upper Bound on the Mass of the Type III Seesaw Triplet in an SU(5) Model*,” JHEP **06** (2007) 029, [arXiv:hep-ph/0612216](#).

- [21] R. Franceschini, T. Hambye, and A. Strumia, “*Type-III see-saw at LHC*,” Phys. Rev. D **78** (2008) 033002, arXiv:0805.1613.
- [22] X.-G. He and S. Oh, “*Lepton FCNC in Type III Seesaw Model*,” JHEP **09** (2009) 027, arXiv:0902.4082.
- [23] S. F. King and M. Malinsky, “*A(4) family symmetry and quark-lepton unification*,” Phys. Lett. B **645** (2007) 351–357, arXiv:hep-ph/0610250.
- [24] R. Kalita and D. Borah, “*Constraining a type I seesaw model with  $A_4$  flavor symmetry from neutrino data and leptogenesis*,” Phys. Rev. D **92** (2015) no. 5, 055012, arXiv:1508.05466.
- [25] G. Altarelli, “*Lectures on models of neutrino masses and mixings*,” Soryushiron Kenkyu Electron. **116** (2008) A29–A55, arXiv:0711.0161.
- [26] T. Kimura, “*The minimal  $S(3)$  symmetric model*,” Prog. Theor. Phys. **114** (2005) 329–358.
- [27] S. Mishra, “*Majorana dark matter and neutrino mass with  $S_3$  symmetry*,” Eur. Phys. J. Plus **135** (2020) no. 6, 485, arXiv:1911.02255.
- [28] D. Meloni, S. Morisi, and E. Peinado, “*Fritzsch neutrino mass matrix from  $S_3$  symmetry*,” J. Phys. G **38** (2011) 015003, arXiv:1005.3482.
- [29] S. Pramanick, “*Scotogenic  $S_3$  symmetric generation of realistic neutrino mixing*,” Phys. Rev. D **100** (2019) no. 3, 035009, arXiv:1904.07558.
- [30] R. Krishnan, P. F. Harrison, and W. G. Scott, “*Simplest Neutrino Mixing from  $S_4$  Symmetry*,” JHEP **04** (2013) 087, arXiv:1211.2000.
- [31] M. Chakraborty, R. Krishnan, and A. Ghosal, “*Predictive  $S_4$  flavon model with  $TM_1$  mixing and baryogenesis through leptogenesis*,” JHEP **09** (2020) 025, arXiv:2003.00506.
- [32] V. V. Vien, “*Lepton mass and mixing in a neutrino mass model based on  $S_4$  flavor symmetry*,” Int. J. Mod. Phys. A **31** (2016) no. 09, 1650039, arXiv:1603.03933.
- [33] E. Ma and R. Srivastava, “*Dirac or inverse seesaw neutrino masses with  $B - L$  gauge symmetry and  $S_3$  flavor symmetry*,” Phys. Lett. B **741** (2015) 217–222, arXiv:1411.5042.
- [34] S. Kanemura, T. Matsui, and H. Sugiyama, “*Neutrino mass and dark matter from gauged  $U(1)_{B-L}$  breaking*,” Phys. Rev. D **90** (2014) 013001, arXiv:1405.1935.
- [35] S. Kanemura, T. Nabeshima, and H. Sugiyama, “*Radiative type-I seesaw model with dark matter via  $U(1)_{B-L}$  gauge symmetry breaking at future linear colliders*,” Phys. Rev. D **87** (2013) no. 1, 015009, arXiv:1207.7061.
- [36] S. Mishra, S. Singirala, and S. Sahoo, “*Scalar dark matter, Neutrino mass, Leptogenesis and rare  $B$  decays in a  $U(1)_{B-L}$  model*,” arXiv:1908.09187.
- [37] S. Singirala, R. Mohanta, S. Patra, and S. Rao, “*Majorana Dark Matter in a new  $B - L$  model*,” JCAP **11** (2018) 026, arXiv:1710.05775.
- [38] H. Cai, T. Nomura, and H. Okada, “*A neutrino mass model with hidden  $U(1)$  gauge symmetry*,” Nucl. Phys. B **949** (2019) 114802, arXiv:1812.01240.
- [39] T. Nomura, H. Okada, and P. Sanyal, “*A radiatively induced inverse seesaw model with hidden  $U(1)$  gauge symmetry*,” arXiv:2103.09494.

- [40] U. K. Dey, T. Nomura, and H. Okada, “*Inverse seesaw model with global  $U(1)_H$  symmetry*,” Phys. Rev. D **100** (2019) no. 7, 075013, [arXiv:1902.06205](#).
- [41] A. Esmaili and Y. Farzan, “*Explaining the ANITA events by a  $L_e - L_\tau$  gauge model*,” JCAP **12** (2019) 017, [arXiv:1909.07995](#).
- [42] M. K. Behera, P. Panda, P. Mishra, S. Singirala, and R. Mohanta, “*Exploring Neutrino Masses and Mixing in the Seesaw Model with  $L_e - L_\tau$  Gauged Symmetry*,” [arXiv:2108.04066](#).
- [43] T. Kobayashi, K. Tanaka, and T. H. Tatsuishi, “*Neutrino mixing from finite modular groups*,” Phys. Rev. D **98** (2018) no. 1, 016004, [arXiv:1803.10391](#).
- [44] F. Feruglio, *Are neutrino masses modular forms?*, pp. 227–266. 2019. [arXiv:1706.08749](#).
- [45] R. de Adelhart Toorop, F. Feruglio, and C. Hagedorn, “*Finite Modular Groups and Lepton Mixing*,” Nucl. Phys. B **858** (2012) 437–467, [arXiv:1112.1340](#).
- [46] E. Dudas, S. Pokorski, and C. A. Savoy, “*Soft scalar masses in supergravity with horizontal  $U(1)$ - $x$  gauge symmetry*,” Phys. Lett. B **369** (1996) 255–261, [arXiv:hep-ph/9509410](#).
- [47] G. K. Leontaris and N. D. Tracas, “*Modular weights,  $U(1)$ ’s and mass matrices*,” Phys. Lett. B **419** (1998) 206–210, [arXiv:hep-ph/9709510](#).
- [48] X. Du and F. Wang, “*SUSY breaking constraints on modular flavor  $S_3$  invariant  $SU(5)$  GUT model*,” JHEP **02** (2021) 221, [arXiv:2012.01397](#).
- [49] S. Mishra, “*Neutrino mixing and Leptogenesis with modular  $S_3$  symmetry in the framework of type III seesaw*,” [arXiv:2008.02095](#).
- [50] H. Okada and Y. Orikasa, “*Modular  $S_3$  symmetric radiative seesaw model*,” Phys. Rev. D **100** (2019) no. 11, 115037, [arXiv:1907.04716](#).
- [51] J. Penedo and S. Petcov, “*Lepton Masses and Mixing from Modular  $S_4$  Symmetry*,” Nucl. Phys. B **939** (2019) 292–307, [arXiv:1806.11040](#).
- [52] P. Novichkov, J. Penedo, S. Petcov, and A. Titov, “*Modular  $S_4$  models of lepton masses and mixing*,” JHEP **04** (2019) 005, [arXiv:1811.04933](#).
- [53] H. Okada and Y. Orikasa, “*Neutrino mass model with a modular  $S_4$  symmetry*,” [arXiv:1908.08409](#).
- [54] M. Abbas, “*Modular  $A_4$  Invariance Model for Lepton Masses and Mixing*,” Phys. Atom. Nucl. **83** (2020) no. 5, 764–769.
- [55] K. I. Nagao and H. Okada, “*Lepton sector in modular  $A_4$  and gauged  $U(1)_R$  symmetry*,” [arXiv:2010.03348](#).
- [56] T. Asaka, Y. Heo, and T. Yoshida, “*Lepton flavor model with modular  $A_4$  symmetry in large volume limit*,” Phys. Lett. B **811** (2020) 135956, [arXiv:2009.12120](#).
- [57] T. Nomura and H. Okada, “*A linear seesaw model with  $A_4$ -modular flavor and local  $U(1)_{B-L}$  symmetries*,” [arXiv:2007.04801](#).
- [58] H. Okada and Y. Shoji, “*A radiative seesaw model with three Higgs doublets in modular  $A_4$  symmetry*,” Nucl. Phys. B **961** (2020) 115216, [arXiv:2003.13219](#).

- [59] M. K. Behera, S. Singirala, S. Mishra, and R. Mohanta, “*A modular  $A_4$  symmetric scotogenic model for neutrino mass and dark matter,*” J. Phys. G **49** (2022) no. 3, 035002, [arXiv:2009.01806](#).
- [60] M. K. Behera and R. Mohanta, “*Inverse seesaw in  $A'_5$  modular symmetry,*” J. Phys. G **49** (2022) no. 4, 045001, [arXiv:2108.01059](#).
- [61] M. K. Behera, S. Mishra, S. Singirala, and R. Mohanta, “*Implications of  $A_4$  modular symmetry on Neutrino mass, Mixing and Leptogenesis with Linear Seesaw,*” [arXiv:2007.00545](#).
- [62] G.-J. Ding, S. F. King, and X.-G. Liu, “*Modular  $A_4$  symmetry models of neutrinos and charged leptons,*” JHEP **09** (2019) 074, [arXiv:1907.11714](#).
- [63] G. Altarelli and F. Feruglio, “*Tri-bimaximal neutrino mixing,  $A(4)$  and the modular symmetry,*” Nucl. Phys. B **741** (2006) 215–235, [arXiv:hep-ph/0512103](#).
- [64] P. Novichkov, J. Penedo, S. Petcov, and A. Titov, “*Modular  $A_5$  symmetry for flavour model building,*” JHEP **04** (2019) 174, [arXiv:1812.02158](#).
- [65] M. Kashav and S. Verma, “*Broken scaling neutrino mass matrix and leptogenesis based on  $A_4$  modular invariance,*” JHEP **09** (2021) 100, [arXiv:2103.07207](#).
- [66] C.-Y. Yao, X.-G. Liu, and G.-J. Ding, “*Fermion masses and mixing from the double cover and metaplectic cover of the  $A_5$  modular group,*” Phys. Rev. D **103** (2021) no. 9, 095013, [arXiv:2011.03501](#).
- [67] L. L. Everett and A. J. Stuart, “*The Double Cover of the Icosahedral Symmetry Group and Quark Mass Textures,*” Phys. Lett. B **698** (2011) 131–139, [arXiv:1011.4928](#).
- [68] K. Hashimoto and H. Okada, “*Lepton Flavor Model and Decaying Dark Matter in The Binary Icosahedral Group Symmetry,*” [arXiv:1110.3640](#).
- [69] C.-S. Chen, T. W. Kephart, and T.-C. Yuan, “*Binary Icosahedral Flavor Symmetry for Four Generations of Quarks and Leptons,*” PTEP **2013** (2013) no. 10, 103B01, [arXiv:1110.6233](#).
- [70] X. Wang, B. Yu, and S. Zhou, “*Double covering of the modular  $A_5$  group and lepton flavor mixing in the minimal seesaw model,*” Phys. Rev. D **103** (2021) no. 7, 076005, [arXiv:2010.10159](#).
- [71] W. Grimus, “*Theory of Neutrino Masses and Mixing,*” Phys. Part. Nucl. **42** (2011) 566–576, [arXiv:1101.0137](#).
- [72] E. Ma, “*Neutrino Mass: Mechanisms and Models,*” [arXiv:0905.0221](#).
- [73] M. Sruthilaya, R. Mohanta, and S. Patra, “ *$A_4$  realization of Linear Seesaw and Neutrino Phenomenology,*” Eur. Phys. J. C **78** (2018) no. 9, 719, [arXiv:1709.01737](#).
- [74] D. Borah and B. Karmakar, “*Linear seesaw for Dirac neutrinos with  $A_4$  flavour symmetry,*” Phys. Lett. B **789** (2019) 59–70, [arXiv:1806.10685](#).
- [75] D. Borah and B. Karmakar, “ *$A_4$  flavour model for Dirac neutrinos: Type I and inverse seesaw,*” Phys. Lett. B **780** (2018) 461–470, [arXiv:1712.06407](#).

- [76] S. Dawson, “*Electroweak Symmetry Breaking and Effective Field Theory*,” in *Theoretical Advanced Study Institute in Elementary Particle Physics: Anticipating the Next Discoveries in Particle Physics*, pp. 1–63. 12, 2017. [arXiv:1712.07232](#).
- [77] **KamLAND-Zen**, A. Gando *et al.*, “*Search for Majorana Neutrinos near the Inverted Mass Hierarchy Region with KamLAND-Zen*,” *Phys. Rev. Lett.* **117** (2016) no. 8, 082503, [arXiv:1605.02889](#). [Addendum: *Phys.Rev.Lett.* 117, 109903 (2016)].
- [78] P. de Salas, D. Forero, C. Ternes, M. Tortola, and J. Valle, “*Status of neutrino oscillations 2018:  $3\sigma$  hint for normal mass ordering and improved CP sensitivity*,” *Phys. Lett. B* **782** (2018) 633–640, [arXiv:1708.01186](#).
- [79] S. Gariazzo, M. Archidiacono, P. de Salas, O. Mena, C. Ternes, and M. Tórtola, “*Neutrino masses and their ordering: Global Data, Priors and Models*,” *JCAP* **03** (2018) 011, [arXiv:1801.04946](#).
- [80] I. Esteban, M. Gonzalez-Garcia, A. Hernandez-Cabezudo, M. Maltoni, and T. Schwetz, “*Global analysis of three-flavour neutrino oscillations: synergies and tensions in the determination of  $\theta_{23}$ ,  $\delta_{CP}$ , and the mass ordering*,” *JHEP* **01** (2019) 106, [arXiv:1811.05487](#).
- [81] **Planck**, N. Aghanim *et al.*, “*Planck 2018 results. V. CMB power spectra and likelihoods*,” *Astron. Astrophys.* **641** (2020) A5, [arXiv:1907.12875](#).
- [82] **Planck**, N. Aghanim *et al.*, “*Planck 2018 results. VI. Cosmological parameters*,” *Astron. Astrophys.* **641** (2020) A6, [arXiv:1807.06209](#). [Erratum: *Astron.Astrophys.* 652, C4 (2021)].
- [83] D. V. Forero, S. Morisi, M. Tortola, and J. W. F. Valle, “*Lepton flavor violation and non-unitary lepton mixing in low-scale type-I seesaw*,” *JHEP* **09** (2011) 142, [arXiv:1107.6009](#).
- [84] S. Antusch and O. Fischer, “*Non-unitarity of the leptonic mixing matrix: Present bounds and future sensitivities*,” *JHEP* **10** (2014) 094, [arXiv:1407.6607](#).
- [85] M. Blennow, P. Coloma, E. Fernandez-Martinez, J. Hernandez-Garcia, and J. Lopez-Pavon, “*Non-Unitarity, sterile neutrinos, and Non-Standard neutrino Interactions*,” *JHEP* **04** (2017) 153, [arXiv:1609.08637](#).
- [86] E. Fernandez-Martinez, J. Hernandez-Garcia, and J. Lopez-Pavon, “*Global constraints on heavy neutrino mixing*,” *JHEP* **08** (2016) 033, [arXiv:1605.08774](#).
- [87] A. Sakharov, “*Violation of CP Invariance, C asymmetry, and baryon asymmetry of the universe*,” *Sov. Phys. Usp.* **34** (1991) no. 5, 392–393.
- [88] A. Pilaftsis, “*CP violation and baryogenesis due to heavy Majorana neutrinos*,” *Phys. Rev. D* **56** (1997) 5431–5451, [arXiv:hep-ph/9707235](#).
- [89] G. Bambhaniya, P. Bhupal Dev, S. Goswami, S. Khan, and W. Rodejohann, “*Naturalness, Vacuum Stability and Leptogenesis in the Minimal Seesaw Model*,” *Phys. Rev. D* **95** (2017) no. 9, 095016, [arXiv:1611.03827](#).

- [90] A. Pilaftsis and T. E. Underwood, “*Resonant leptogenesis*,” Nucl. Phys. B **692** (2004) 303–345, [arXiv:hep-ph/0309342](#).
- [91] A. Abada, G. Arcadi, V. Domcke, M. Drewes, J. Klaric, and M. Lucente, “*Low-scale leptogenesis with three heavy neutrinos*,” JHEP **01** (2019) 164, [arXiv:1810.12463](#).
- [92] A. Pilaftsis and T. E. Underwood, “*Electroweak-scale resonant leptogenesis*,” Phys. Rev. D **72** (2005) 113001, [arXiv:hep-ph/0506107](#).
- [93] T. Asaka and T. Yoshida, “*Resonant leptogenesis at TeV-scale and neutrinoless double beta decay*,” JHEP **09** (2019) 089, [arXiv:1812.11323](#).
- [94] P.-H. Gu and U. Sarkar, “*Leptogenesis with Linear, Inverse or Double Seesaw*,” Phys. Lett. B **694** (2011) 226–232, [arXiv:1007.2323](#).
- [95] S. Davidson, E. Nardi, and Y. Nir, “*Leptogenesis*,” Phys. Rept. **466** (2008) 105–177, [arXiv:0802.2962](#).
- [96] W. Buchmuller, P. Di Bari, and M. Plumacher, “*Leptogenesis for pedestrians*,” Annals Phys. **315** (2005) 305–351, [arXiv:hep-ph/0401240](#).
- [97] M. Plumacher, “*Baryogenesis and lepton number violation*,” Z. Phys. C **74** (1997) 549–559, [arXiv:hep-ph/9604229](#).
- [98] G. Giudice, A. Notari, M. Raidal, A. Riotto, and A. Strumia, “*Towards a complete theory of thermal leptogenesis in the SM and MSSM*,” Nucl. Phys. B **685** (2004) 89–149, [arXiv:hep-ph/0310123](#).
- [99] A. Strumia, “*Baryogenesis via leptogenesis*,” in *Les Houches Summer School on Theoretical Physics: Session 84: Particle Physics Beyond the Standard Model*, pp. 655–680. 8, 2006. [arXiv:hep-ph/0608347](#).
- [100] S. Iso, N. Okada, and Y. Orikasa, “*Resonant Leptogenesis in the Minimal B-L Extended Standard Model at TeV*,” Phys. Rev. D **83** (2011) 093011, [arXiv:1011.4769](#).
- [101] S. Pascoli, S. T. Petcov, and A. Riotto, “*Leptogenesis and Low Energy CP Violation in Neutrino Physics*,” Nucl. Phys. B **774** (2007) 1–52, [arXiv:hep-ph/0611338](#).
- [102] S. Antusch, S. F. King, and A. Riotto, “*Flavour-Dependent Leptogenesis with Sequential Dominance*,” JCAP **11** (2006) 011, [arXiv:hep-ph/0609038](#).
- [103] E. Nardi, Y. Nir, E. Roulet, and J. Racker, “*The Importance of flavor in leptogenesis*,” JHEP **01** (2006) 164, [arXiv:hep-ph/0601084](#).
- [104] A. Abada, S. Davidson, A. Ibarra, F. X. Josse-Michaux, M. Losada, and A. Riotto, “*Flavour Matters in Leptogenesis*,” JHEP **09** (2006) 010, [arXiv:hep-ph/0605281](#).
- [105] A. Granelli, K. Moffat, and S. T. Petcov, “*Flavoured resonant leptogenesis at sub-TeV scales*,” Nucl. Phys. B **973** (2021) 115597, [arXiv:2009.03166](#).
- [106] P. S. B. Dev, P. Di Bari, B. Garbrecht, S. Lavignac, P. Millington, and D. Teresi, “*Flavor effects in leptogenesis*,” Int. J. Mod. Phys. A **33** (2018) 1842001, [arXiv:1711.02861](#).
- [107] D. Schultz, “*Notes on modular forms*,” <https://faculty.math.illinois.edu/schult25/ModFormNotes.pdf>.

- [108] G.-J. Ding, S. F. King, and X.-G. Liu, “*Neutrino mass and mixing with  $A_5$  modular symmetry,*” *Phys. Rev. D* **100** (2019) no. 11, 115005, [arXiv:1903.12588](#).